Application of a Computational Fluid Dynamics Model to the Preliminary Hydraulic Design of Pump Stations S332B and S332C

Jie Zeng, Matahel Ansar and Zubayed Rakib

November 2018

APPLIED HYDRAULICS SECTION
HYDROLOGY AND HYDRAULICS BUREAU
SOUTH FLORIDA WATER MANAGEMENT DISTRICT

EXECUTIVE SUMMARY

This report presents an application of Computational Fluid Dynamics (CFD) to the preliminary hydraulic design of replacement pump stations for interim pump stations S332B and S332C. During the operations and maintenance of existing S332B and S332C temporary pump stations, some design limitations became apparent over time. According to the "Structure Inspection Report as part of the Structure Inspection Program (2013)", the construction of S332B and S332C did not adhere to District standards as the pump stations were meant to be temporary in nature only. Additionally, the inflow canal for each structure is oriented at 90° to the pump intakes, causing the inflow field to be biased towards one side of the intakes. The imbalance of the flow field not only decrease pump efficiency but also causes potential vibration issues. Moreover, biased inflows can cause formation of vortices and swirls, that can lead to mechanical failure of pump components. As a result of these factors, District staff had to perform frequent repairs and maintenance work to address abnormal pump noise, worn bearings, leaking seals and high levels of corrosion. The S332B and S332C redesign / relocation project consists of relocating the existing pump stations to ensure a balanced flow field at the pump intake, acceptable hydraulic efficiencies, and the minimization of potential vibration and noise issues. To evaluate these issues the current CFD flow analysis includes layout and scenario evaluations. More specifically, the analyses focus on the evaluation of different design scenarios and provide recommendations to improve the flow fields and hydrodynamic performance of the approaching canal and pump unit forebays.

In developing the CFD models, three-dimensional geometries of the approaching canal, forebays, and pump intakes for S332B and S332C were prepared first along with the associated high-quality meshes. The setup of numerical solution in *FLUENT* included determining simulation domain, defining boundary conditions, prescribing initial conditions and time step, and setting up the convergence criteria.

The established CFD models were applied first to the evaluation of existing conditions at S332B and S332C. Proposed design scenarios to address the existing problems were then investigated to support the relocation and redesign of the existing structures. Based on a selected location and layout of the new and relocated pump stations, various CFD simulations were

conducted. Initially CFD simulations were intended to be carried out for three different operation plans: Everglades Restoration Transition Plan 2012 (ERTP), South Dade Investigation, and Central Everglades Planning Project (CEPP). However, after detailed analysis of historical and model runs data, boundary conditions that are all encompassing and more restrictive than those corresponding to the three operation plans were selected. The investigation focused on the simulation of turbulence/unsteadiness in the approach flow, free-surface vortices, flow pre-swirl, non-uniform velocity profiles at the throat of the pump suction bell, etc.

The CFD analysis indicated that the inflow to each existing pump station is directionally biased. Similarly, inflows to each of the relocated pump stations will be directionally biased if flow separating vanes are not incorporated into the design. The approaching flow and pre-swirl conditions, however, significantly improve with the installation of flow separating vanes and trash rack. Further optimization of the location of each pump station and the arrangement of its individual pumps and vanes is needed during subsequent design phases.

Based on the CFD simulations, the recommended location of the new S332B and S332C pump stations is 300 ft downstream along L-31 canal and 300 ft further west from their respective current locations, with four diesel units (125 cfs each) in the center and two electric units (75 cfs each) placed on each end. Flow separating vanes and trash rack are recommended to ensure even approach flow distributions, even velocity distributions at the throat of pump suction bells, and minimal flow pre-swirl in the pump column. For both S332B and S332C pump stations, one electric pump unit (75 cfs) is provided as redundancy.

ACKNOWLEDGEMENT

The authors of this report would like to thank Mark Wilsnack and Brenda Mills for reviewing and proof reading this document.

TABLE OF CONTENTS

INTRODUCTION AND BACKGROUND 7
Introduction 7
S332B 7
S332C 7
Pump Station Issues 8
OBJECTIVES 8
CFD MODEL BACKGROUND 9
Literature Review on CFD Applications 9
Introduction to CFD Software 11
CFD MODELING OF PUMP STATIONS 12
Structure Configuration, Model Boundary Conditions, Mesh Generation 12
Model Development and Validation 14
Application of CFD Model for Scenarios Study 14
Evaluation of Selected Pump Layout with Different Pump Operation Plans 16
Design Criteria for Pump Intake 17
RESULTS OF CFD MODEL SIMULATIONS 18
SCENARIO 1 18
S332B Existing Conditions 18
S332B Proposed Conditions 22
Model Simulations Without a Trash Rack 22
Model Simulations with a Trash Rack 25
S332C Existing Condition 28
S332C Proposed Condition 32
Model Simulations Without a Trash Rack 32
Model Simulations with a Trash Rack 36
SCENARIO 2 40
S332B Proposed Condition 40
S332C Proposed Condition 44
SUMMARY 48
REFERENCES 49
APPENDIX 51

INTRODUCTION AND BACKGROUND

Introduction

S332B and S332C pump stations are located along the L-31N canal, south of Pump Station 331. Their primary purpose is to transfer excess water from the L-31N borrow canal to the South Detention Area (SDA) located within the eastern Everglades National Park (ENP). Since 2004, a number of operation and maintenance issues with these structures have become apparent. These include pump vibrations, loss of capacity and degradation of pump discharge lines. Since these pump stations have already surpassed their intended service life, the U.S. Army Corps of Engineers (USACE) has proposed the construction of permanent and relocated pump stations. In order to ensure the hydrodynamic performance of these new pump stations, a Computational Fluid Dynamics (CFD) based analysis of the proposed pump station intake facilities was performed to develop a preliminary pump station alignment and arrangement of individual pump units.

S332B

Structure S332B is a five-unit pump station. Its construction began on January 29, 2000 and was completed April 12, 2000. The structure is operated as directed by the USACE and can be operated remotely from the S-331 pump station. S332B transfers excess flows in the L-31N borrow canal to the South Detention Area (SDA) and North Detention Area (NDA) through buried conduits. The minimum L-31N pumping stage is 3.0 feet NGVD. The total structure capacity is 575 cfs (4 x 125 cfs diesel units, and 1 x 75 cfs electric unit). Additional information is provided in the Appendix.

S332C

Pump station S332C is a component of alternative 7R for the Interim Operational Plan (IOP) within the C-111 basin. Its functional purposes are similar to those of S332B in that it transfers water from the C-111 borrow canal to a detention basin located within the eastern ENP. It is equipped with 5 vertical, axial-flow pumps mounted on an outdoor platform. Four are driven by diesel engines with a nominal design speed of 1800 RPM. The fifth is driven by an electric motor with a nominal speed of 1785 RPM. The discharge pipes for all pumps extend approximately one half a mile into the ENP and terminate at the associated detention reservoir.

Pump Station Issues

Since 2004, issues related to the operation and maintenance of S332B and S332C have been arising. According to the "Structure Inspection Report as part of the Structure Inspection Program (2013)", the construction of S332B and S332C did not adhere to District standards since the pump stations were meant to be temporary in nature only. Issues related to pump vibration, loss of capacity and degradation of pump discharge lines warranted the District staff to perform frequent repairs and maintenance work on each pump station. Furthermore, the Structure Inspection Report also states that the underground CMPs connecting the S332B and S332C pump discharge pipes to the detention areas tend to leak, are problematic to maintain, and have high levels of corrosion.

During the dry season, large rainfall events sometimes increase the L-31N canal stage at the structures above 5 ft-NGVD. In general, though, there appears to be excess capacity at each of the S332B and S332C pump station. This extra capacity could be utilized as part of a test to assess whether it is possible to lower the water level in the L-31N canal during the dry season while maintaining the hydrological benefits in the Everglades National Park (ENP). This operation would, however, likely increase the seepage return rate and the need for additional pumping to compensate. Any allowances to lower the L-31N canal stage are, unfortunately, constrained by the current water supply level (4.0 ft-NGVD) along with the competing effects of pumping rate versus the seepage return rate.

Currently, the L-31N borrow canal at S332B and S332C is oriented at 90° to the pump units. This causes the flow field to be biased to one side of the pump intakes. The imbalance of the flow field does not only decrease pump efficiency but also causes potential vibration issues. Moreover, biased inflows can cause formation of vortices and swirls that can cause mechanical failure of the pump propellers and other pump components. Based on pump operation experience, one of the recommendations for the replacement of the S332B and S332C pump stations is to reorient the diesel exhaust pipes towards the west from the existing locations.

OBJECTIVES

This objective of this study is to use Computational Fluid Dynamics (CFD) models to evaluate the proposed design and relocation of S332B and S332C. The CFD studies include: i) an evaluation of the impacts of the current unbalanced inflow fields on the performance of S332B

and S332C and associated vibration issues; and ii) assessments of the proposed relocations and realignment of the structures along with proposed pump unit locations and configurations.

Traditionally, reduced-scale physical models have been used for this type of investigation. While this approach is generally the most reliable, it is also the costliest and time consuming. In this study, instead of relying on physical models, CFD model simulations will be used to investigate the complex three-dimensional flow physics of pump intake facilities, including pressure and velocity fields, turbulent intensity, vorticity, and fluid-structure interactions. The analyses focus on the evaluation of different design and structure location scenarios and provide recommendations to improve flow fields within the approaching canals and forebays at S332B and S332C. Additionally, the CFD analyses will help screen design alternatives for further testing in a physical model. Recommendations for minimizing the pump vibration problems are provided.

The aforementioned objectives are summarized as follows:

1. Perform a CFD analysis to examine current existing conditions of the flow fields within the approach canal, the forebays, and pump intakes of S332B and S332C to understand current design deficiencies
2. Perform CFD analyses to examine the proposed scenarios for structure location, structure alignment, and pump arrangement in order to ensure favorable inflow hydrodynamics
3. Based on proposed layout of pump station S332B and S332C, further CFD simulations will be conducted to satisfy the corresponding to 2012 Everglades Restoration Transition Plan (ERTP) and Central Everglades Planning Project (CEPP) operation plans requirement. Investigation will focus on the simulation of the turbulence/unsteadiness of the approaching flows, vorticities, swirl, non-uniform velocity profiles, etc. and resolve any adverse hydraulic conditions which may lead to decreased hydraulic efficiency, abnormal pump noise and vibration, and mechanical failure of pump components.
4. Provide a recommended design scenario to build upon for further analysis in the final design phase.

CFD MODEL BACKGROUND

Literature Review on CFD Applications

In recent years, advancements in Computational Fluid Dynamics (CFD) have enabled

numerical modeling to be practical for the analysis of fluid flows. Large eddy simulation (LES) and detached eddy simulation (DES) turbulence models used in CFD can provide very accurate results. However, they are time intensive and can require substantial computational resources, limiting their application to engineering problems. Steady/unsteady Reynolds-Averaged Navier-Stokes (*RANS*) models with advanced turbulence closures, without the limitations introduced by the popular wall-function approach, offer the most economic approach for computing complex turbulent flows. These models are not only cost and resource effective, but also suitable for many hydraulic engineering applications (Nielsen and Diskin, 2017). For example, *RANS* turbulence models have been applied to examine the flow physics of natural river reaches containing complex hydraulic structures to address scour and deposition patterns (Ge and Sotiropoulos, 2005; Ge *et al*., 2005). Zhao *et al*. (2004) successfully applied the two-dimensional k-ε turbulence model and volume of fluid (VOF) method for free surface location and horizontal velocity to study the hydraulic jump theory on a smooth bed.

Tagomori and Gotoh (1989) employed the finite volume method to solve the *RANS* equations in conjunction with the standard k-ε turbulence model. They studied the effect of non-uniformity in the approach flow on the generation of various types of vortices. Takata *et al*. (1992) was the first to use LES to simulate flow in a pump intake at Reynolds numbers between $1.5\text{x}10^4$ and $5.5\text{x}10^4$. They employed the standard Smagorinsky model with a constant coefficient to relate the sub-grid stresses to the rate of strain of the resolvable scales and wall functions. Lu et al. (1997) solved the *RANS* equations in conjunction with the standard k-ε model and wall functions. They investigated the effect of wall clearances and pump bell shape on the level of velocity distribution uniformity inside the pump column and bay. Ansar (1997) conducted a numerical study of two pump intake geometries, one containing a single pump column and the other containing two pump columns. His work aimed to determine the reliability of a simple inviscid model in predicting flow structures in the approach flow channel of water intakes and the formation of vortices near the suction pipe by comparing the numerical results with the experimental data collected on a model pump intake as part of the same study. Another study by Constantinescu and Patel (1998) developed a *RANS* based model with near-wall modeling capabilities that can be used to improve design methods needed to avoid the formation of strong free surface and subsurface vortices in pump intakes. Constantinescu and Patel (2000) continued with their work by performing another study on pump intake modeling, where the primary goal was to observe the sensitivity of outcomes

of pump intake simulations for different turbulent closure models. In the study by Li *et al*. (2001), a general CFD *RANS* code that can use structured or unstructured multi-block meshes, U^2RANS, was used to simulate three test cases of different complexity including the flow in a pump intake of very complex geometry. Tokyay & Constantinescu (2006) simulated a pressurized pump intake using more realistic intake geometry, where the LES solver was used along with the Dynamic Smagorinsky turbulent closure model. CFD haS also been applied to horizontal pump intake systems (Pradeep *et al*., 2012).

Rajendran et al. (1999) indicate that there are two issues that need to be addressed before CFD can be effectively applied to practical pump intake systems. Firstly, CFD models have to be more robust to handle the complex geometry of pump intakes, such as multiple pumps, partition walls, corner fillets, screens, and other flow-training devices. Secondly, CFD models have to be improved to more accurately capture complex hydrodynamic phenomena such as turbulence, unsteadiness of flows, and free surface effects. Recently, Zhang and Yee (2018) presented a comprehensive review of extent, capacity and possibilities of CFD as a design tool for pump intakes.

Introduction to CFD Software

By solving the Reynolds Averaged Navier-Stokes (*RANS*) equations on a generated 2D or 3D mesh, CFD allows to the simulation of complex three-dimensional flow fields. In the following sections, the CFD model features and model setup used in this study are introduced.

The parallel, pressure-based, non-hydrostatic commercial code ANSYS *FLUENT* was employed as the *RANS* solver in this study. The implicit *RANS* solver, capable of using a hybrid unstructured mesh, employs a cell-centered finite-volume scheme, in which the gradients of the variables are computed by the Green-Gauss' theorem. The second order upwind scheme was used for discretization of the convective terms and the second order accurate central scheme was applied to the diffusion terms. The pressure-implicit split-operator (*PISO*) pressure-velocity coupled algorithm was used to solve the continuity equation.

For the CFD simulations conducted herein, the k-ε turbulence closure model was chosen because it was found to be robust for the various initial conditions of the simulations conducted herein. The transport equations for the k-ε model (k is the turbulent kinetic energy and ε is the turbulence dissipation) are as follows:

$$\frac{\partial}{\partial t}(\rho k) + \frac{\partial}{\partial x_j}(\rho u_j k) = \frac{\partial}{\partial x_j}\left(\frac{\mu_e}{\sigma_k}\frac{\partial k}{\partial x_j}\right) + G_k - \rho\varepsilon$$

$$\frac{\partial}{\partial t}(\rho\varepsilon) + \frac{\partial}{\partial x_j}(\rho u_j \varepsilon) = \frac{\partial}{\partial x_j}\left(\frac{\mu_e}{\sigma_\varepsilon}\frac{\partial \varepsilon}{\partial x_j}\right) + \frac{\varepsilon}{k}(C_1 G_k - C_2 \rho\varepsilon)$$

In the preceding equations, $G_k = -\rho u_i u_j (\partial U_i / \partial x_j)$ is the generation of the turbulent kinetic energy from the mean velocity gradients, and σ_k, σ_ε, C_1 and C_2 are the *k-ε* turbulent model constants. The model constants have the following default values: C_1= 1.44, C_2= 1.92, C_μ= 0.09, σ_k= 1.0 and σ_ε= 1.3. They have been found to work well for a wide range of wall-boundaries and free shear flow (*FLUENT* Manual, Version 13; Zeng *et al*. 2016). The turbulent viscosity, μ_t is obtained from (C_μ= 0.09):

$$\mu_t = \rho C_\mu \frac{k^2}{\varepsilon}$$

CFD MODELING OF PUMP STATIONS

Structure Configuration, Model Boundary Conditions, Mesh Generation

For each proposed pump station, a three-dimensional geometric model that included the approaching canal, forebay, pump intakes and high-quality mesh were prepared first. The proposed pump stations have a design capacity of 650 cfs, which includes 4 diesel pumps (125 cfs each) and 2 electric pumps (75 cfs each). The electric pumps are placed on both ends. The 3D configuration preparation and mesh generation included:

1) Creating a structure geometry using CAD software or other software,
2) Importing the CAD model into pre-processor and preparing CFD mesh for all alternatives considered.

Figure 1, Figure 2, and Figure 3 show the three-dimensional configuration and mesh generation of the pump stations. The canal bottom is set at -10 ft-NGVD based on as-builts. The forebay is extended 50 ft, with a slope of 1:10. A floor clearance of 2 ft was used (0.3D ≤ C ≤ 0.5D, D is the bell diameter). The backwall clearance was 60 inches (more details in Figure A1). The bottom elevation of forebay is set at -12.5 ft-NGVD.

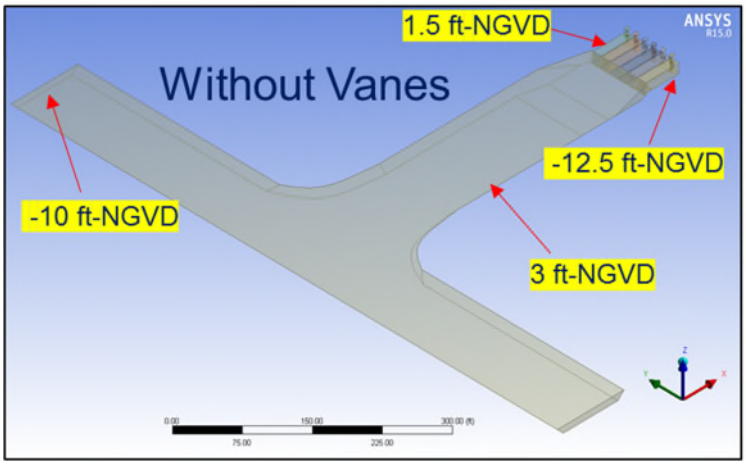

Figure 1. Three-dimensional geometry of pump station and intake channels

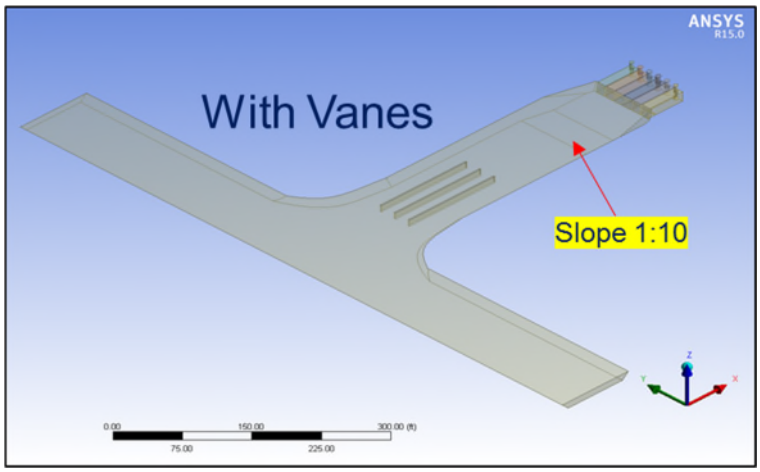

Figure 2. Vanes included in the geometry model

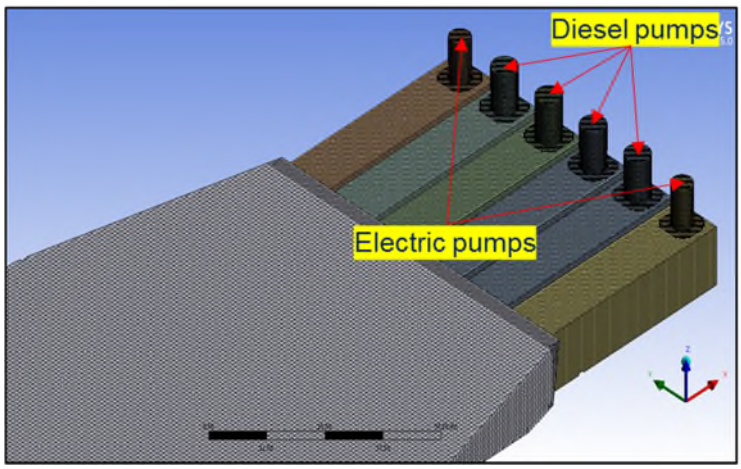

Figure 3. Pump arrangement and mesh generation

Model Development and Validation

CFD model setup in *FLUENT* involves determining simulation domain, defining boundary conditions, generating mesh, prescribing initial conditions and time step, and setting up the convergence criteria. Details on CFD model setup are available in Zeng *et al*. (2016). For brevity, only the main features of the model setup are discussed here.

In this study, the boundary locations were adjusted based on the ability of the flow fields to meet the quasi-uniform, quasi steady flow condition requirements. The boundaries were set at canal stations in relatively straight channel reaches, such that the flow was free from lateral contractions, drawdown effect, and fluctuations induced by large eddies near the canal walls. No slip surfaces were applied for all the solid boundaries including channel bottom, channel banks and walls of the hydraulic structure of the fluid domain. The headwater and tailwater elevations, treated as a pressure inlet and outlet, respectively, were set based on the pump operation plans (discussed in later section). Considered as internal boundaries, the control sections at the structures were monitored during each simulation step. The water surface elevations upstream of, downstream of and within the structures were all set to free-surface. Depending on the cell position, unstructured mesh was used for different zones within the domain based on the equivalent roughness height and velocity estimates near the walls. Smaller mesh sizes were used for the high-velocity domain containing the control sections. For the CFD applications in this study, the total mass flow rate through the control sections, that was continually recorded during the simulation, was used as the indicator for convergence. Convergence was considered achieved when the fluctuations of the mass flow rate at the control section were less than 5% of the average value for the recording period.

The CFD model setup and validation process consisted of the following steps:

1) Setup the CFD model with appropriate geometry and boundary conditions;
2) Perform the detailed 3D CFD analysis with different operations;
3) Post-process the CFD simulations;
4) Perform CFD model validations with benchmark tests or theoretical data analyses, since no field measurement data are available.

Application of CFD Model for Scenarios Study

As indicated previously, the established CFD models were applied first to evaluate existing

conditions at S332B and S332C. The models of the proposed design scenarios were then used to evaluate the various alternatives. Layout alternatives for S332B and S332C are shown in Figure 4 and Figure 5. The existing conditions and design alternatives investigated using CFD simulations are, more specifically:

1. Existing flow conditions at the pump intakes of both S332B and S332C for the situation where all pump units are operating,
2. Future flow conditions at the new and relocated S332B pump station, located about 300 feet downstream along L-31N canal and about 300 feet further west. Flow guiding vanes near the forebay are implemented to avoid imbalance of the inflow field near the pump intake,
3. Future flow conditions at the new and relocated S332C, located further west about 300ft. Flow guiding vanes near the forebay are implemented to avoid imbalance of the inflow field near the pump intake.

Based on field reconnaissance, there are smaller levees within the detention areas, where S332B and C discharge. Thus, the location of the outflow canal of the replaced S332B and S332C pump stations need to connect to the existing smaller canals within the detention area. From these alternatives, Alternative 2 was selected for both pump stations for further CFD analysis. The layout/design of S357 and S332D pump stations were used for reference.

Figure 4. S332B layout alternatives

Figure 5. S332C layout alternatives

Evaluation of Selected Pump Layout with Different Pump Operation Plans

For the selected layout of S332B and S332C, CFD simulations were conducted for boundary conditions that are more restrictive than those specified in 1) South Dade Investigation, 2) Everglades Restoration Transition Plan 2012 (ERTP), and 3) Central Everglades Planning Project (CEPP) as illustrated in Figures 6 and 7. Analysis of historical data and model runs corresponding to these 3 operation plans revealed that running the simulations for a headwater elevations of 3.0 ft NGVD (upstream of the trash rack) and a tailwater elevations of 10 ft NGVD will be more restrictive than all 3 operations plan.

The investigation focused on simulation of phenomena of the turbulence/unsteadiness of approach flow, vortex, swirl, non-uniform velocity profiles, etc. Particular attention was paid to any adverse hydraulic conditions which may cause decreased hydraulic efficiency, abnormal pump noise and vibration, and was resolved. Figures A5 through A8 in the Appendix shows the stage and flows at S332B pump station that were used to determine the boundary conditions for the CFD simulations.

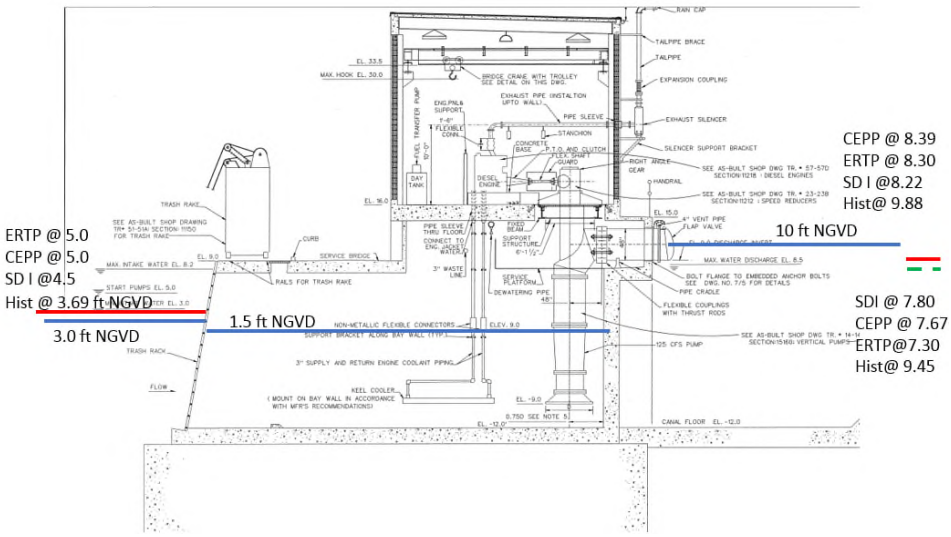

Figure 6. S332B study matrix for selected simulation scenario. Flow simulation uses HW=3.00 ft-NGVD, TW=10.0 ft NGVD

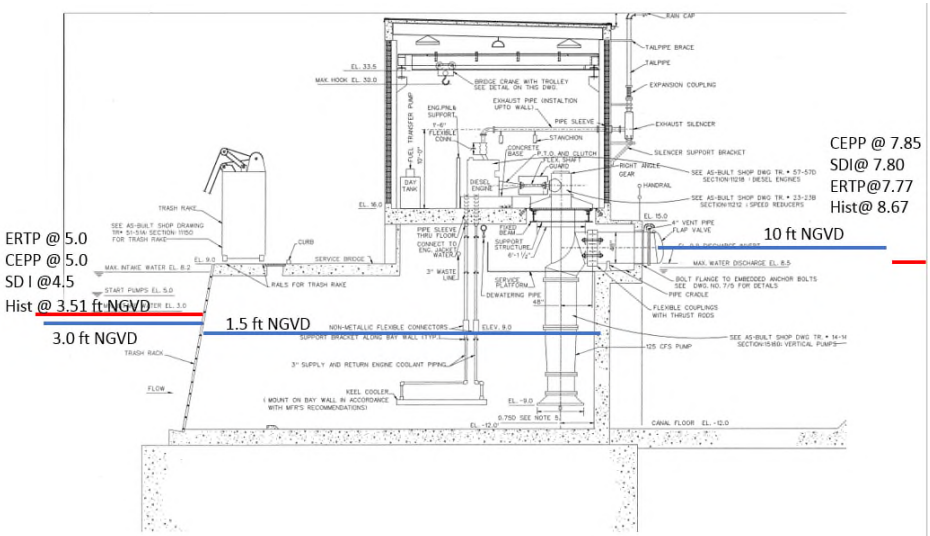

Figure 7. S332C study matrix for selected simulation scenario. Flow simulation uses HW=3.00 ft-NGVD, TW=10.0 ft NGVD

Design Criteria for Pump Intake

The following criteria were considered for the design of the pump intakes at S332B and S332C.

- Approach Flow Patterns
- Free-Surface Vortices
- Sub-Surface Vortices
- Velocity Distribution at the Throat of the Pump Suction Bell
- Flow Pre-swirl

RESULTS OF CFD MODEL SIMULATIONS

For both S332B and S332C pump stations, one electric pump unit (75 cfs) is designed as redundancy. CFD simulations for two operation scenarios were carried out for the proposed pump stations, Scenario 1: all pump units are on (650 cfs), and Scenario 2: one of the electric pump unit is off, reducing the pump capacity to 575 cfs. The recommend design alternative from Scenario 1 was used for Scenario 2 analyses. The following sections describe the results for the two scenarios, starting with simulations of existing conditions followed by the analysis of the proposed design conditions.

SCENARIO 1

S332B Existing Conditions

The simulation of the flow fields within the approach canal, the forebays, and pump intakes for the existing condition at S332B was conducted first to understand the deficiencies in the current design. The existing S332B pump layout contains four diesel units (125 cfs each), and one electric unit (75 cfs) placed in the middle. The CFD simulation was conducted with existing pump station operated at full capacity (575 cfs).

Figure 8 through Figure 13 show the results of the simulations for the existing conditions at S332B pump station. Free surface velocities upstream of the pump station are in the range 0.4-0.6 ft/s, while at downstream is less than 0.10 ft/s. The channel bend north of the pump station causes an increase in velocities and flow bias is also observed near the pump intake in the L-31N canal. This is evident in Figure 8 where the near-bed and near-surface velocity fields are illustrated. Free-surface vortices were not observed.

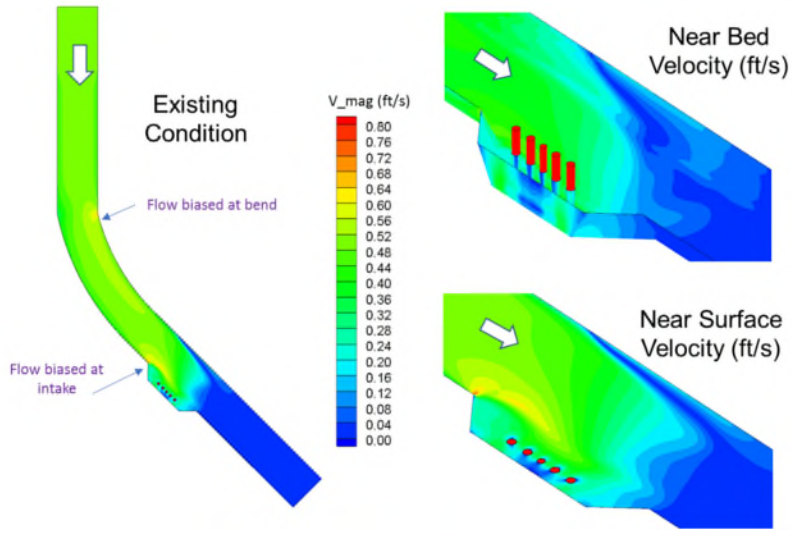

Figure 8. Flow field for existing conditions at S332B

Figure 9 shows the flow lines at the pump station. The approach flow pattern is biased towards the left side of the bank in the L-31N canal. Nearing the intake, the flow sways towards the right side of the channel. This bias would reduce the hydraulic efficiency.

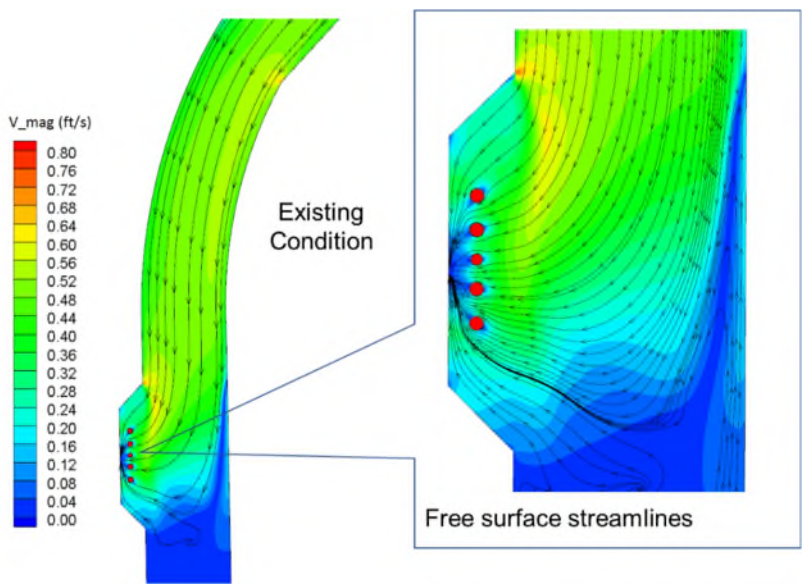

Figure 9. Flow lines, existing conditions at S332B

The cross-section velocity profiles in Figure 10 for existing conditions at S332B display the biased approach flow as well. Sectional velocity profiles at the center of the pumps, shown in Figure 11, indicate that the flow is predominantly in the center of the canal as it approaches the pump columns for both the electric and diesel pumps.

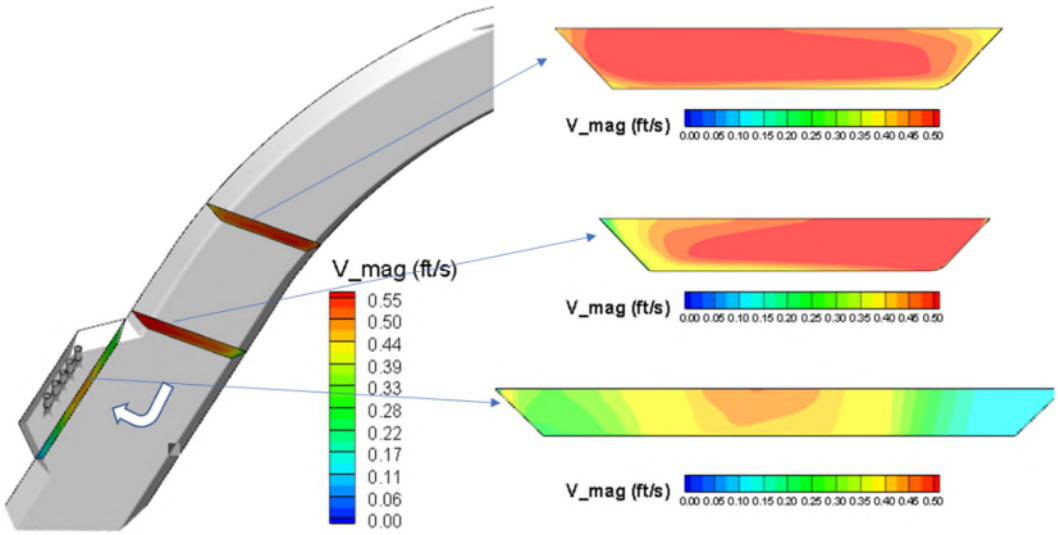

Figure 10. Cross-sectional velocity contours in the approach canal and pump intakes, S332B existing conditions (cross-sections are oriented looking downstream)

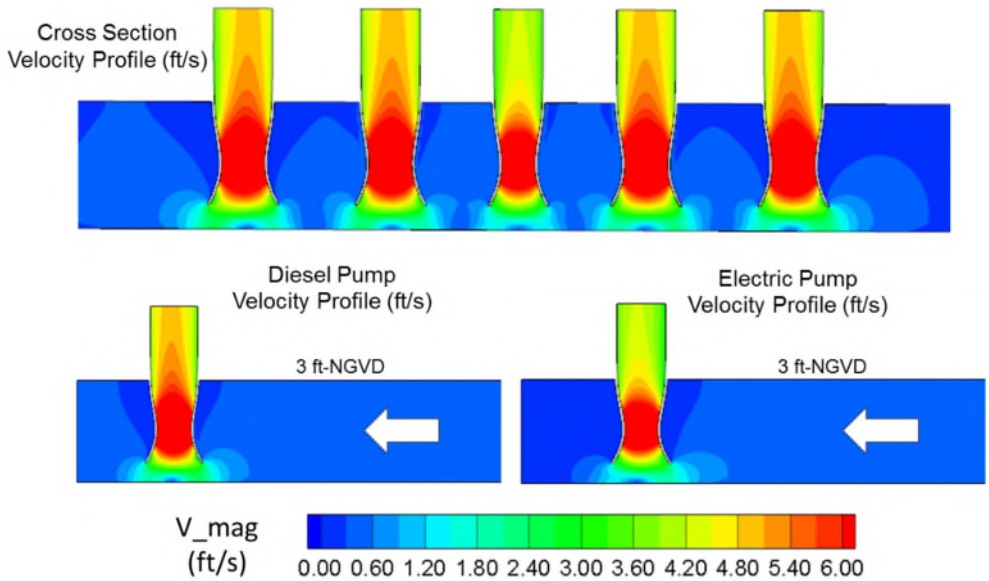

Figure 11. Cross-section velocity profiles, S332B existing condition

The forebay flow velocities approaching the pump bell were about 0.60 ft/s at both the diesel and electric pumps. Since the diesel pumps have higher capacities, the vortex velocities within the intakes of these pumps were higher (5 ft/s). A visualization of the vortices for the existing conditions at S332B using 3D streamlines is shown in Figure 12. The sub-surface vortices can be observed from this figure.

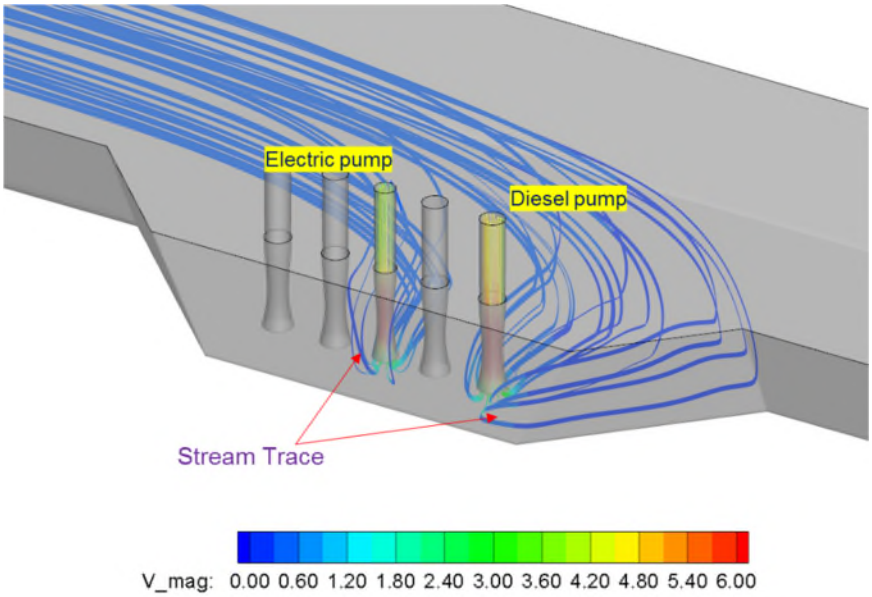

Figure 12. Visualization of vortices using 3D streamlines, S332B existing conditions

Figure 13 shows the axial velocity distribution for the existing condition at S332B pump station. The figure shows that the velocity distribution within the pump suction bell are nearly centered around the vertical axis of symmetry of the pump column. This agrees with the results shown in Figure 11.

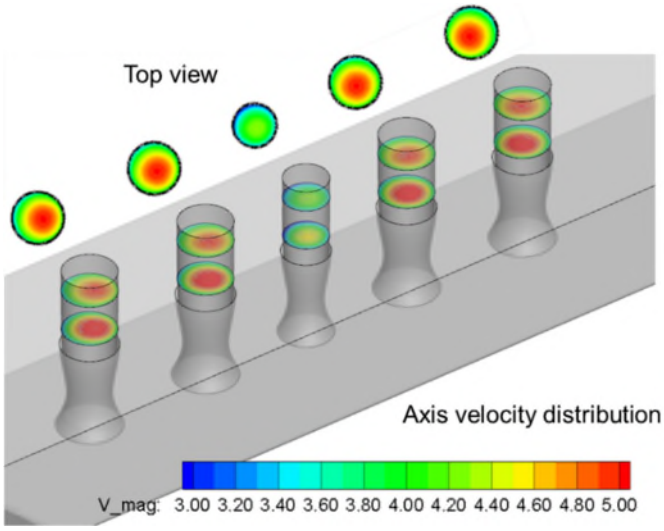

Figure 13. Axis velocity distribution, S332B existing condition

S332B Proposed Conditions

Two set of simulations were conducted for the proposed conditions, namely (i) without a trash rack installed at the entrance of the forebay, and (ii) with a trash rack at this location. In this study, the trash racks were modeled as a porous media (Wang *et al*., 2014). The pressure-drop through the porous media can be written as:

$$\boldsymbol{S} = -\left(\frac{\mu}{k}\boldsymbol{u} + C\frac{1}{2}\rho_o|\boldsymbol{u}|\boldsymbol{u}\right)$$

where, k is the permeability and C is the inertial resistance factor. The first term represents the Darcy's law for laminar flow and the second term is the inertial loss term. Several studies are found in the literature related to determination of C (Geertsma 1974, Carnogurska *et al*. 2012). In this study the Ergun equation (Ergun 1952) was used, and the above equation is expressed as:

$$S = -\left(150\frac{(1-\phi_i)^2\mu}{\varphi_i^3 d_p^2}\boldsymbol{u} + 1.75\frac{(1-\varphi_i)}{\varphi_i^3 d_p}\rho_o|\boldsymbol{u}|\boldsymbol{u}\right)$$

where, the porosity in a cell is the liquid volume fraction of that cell:

$$\phi_i = \frac{V - V_i}{V}$$

In the equation above, V is the total volume and V_i is the volume of the rack components.

Model Simulations Without a Trash Rack

Figure 14 through Figure 19 show the results of the simulations for the proposed conditions that omit the trash rack. Two different simulations were conducted for this scenario, (i) without vanes, and (ii) with vanes. Without vanes, the free surface velocities upstream of the pump station are close to 0.60 ft/s while at downstream in L-31N near the bend is less than 0.10 ft/s. The flow bias at near the entrance to the pump intake channel is strong for this scenario as shown in Figure 14. This leads to an uneven approach flow pattern. The incorporation of vanes into the design resolved this problem, as is evident in Figure 15. The flow bias reduces due to the vanes, and discharge is directed evenly towards the pump intake. The improvement in the flow distribution can be seen from the near surface velocity field.

Figure 16 shows the streamlines approaching S332B under the proposed conditions with vanes. Straight streamlines, indicative of more uniformly distributed flow, are obtained with the vanes included in the design. It is also evident that forebay flows approaching the pump bells are even. This is also evident in the associated cross-section velocity profiles shown in Figure 17.

These unbiased flow distributions should help attain higher hydraulic pump efficiencies.

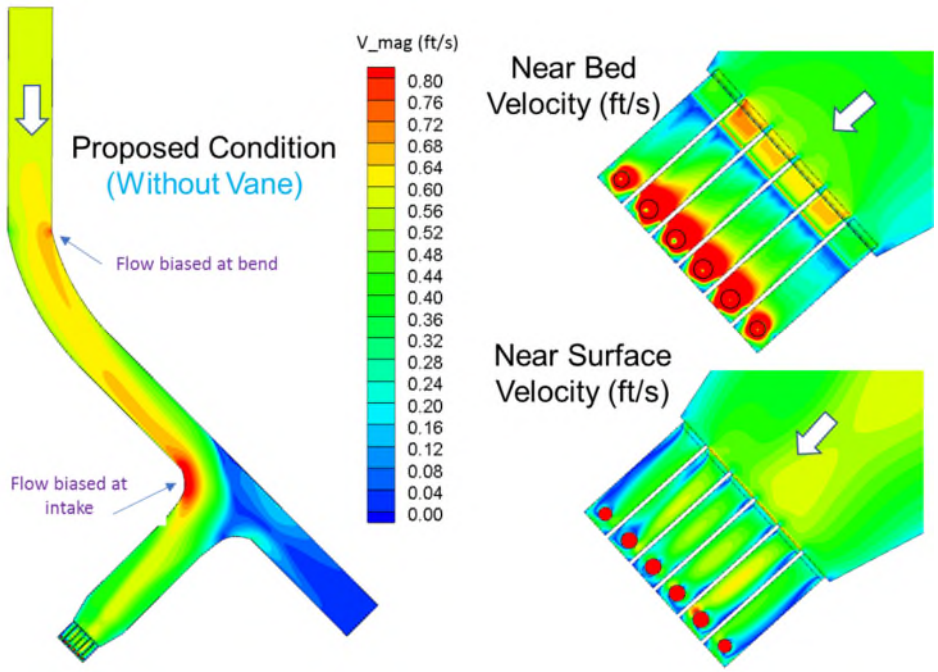

Figure 14. Flow field for the proposed design conditions at S332B without vanes, Scenario 1

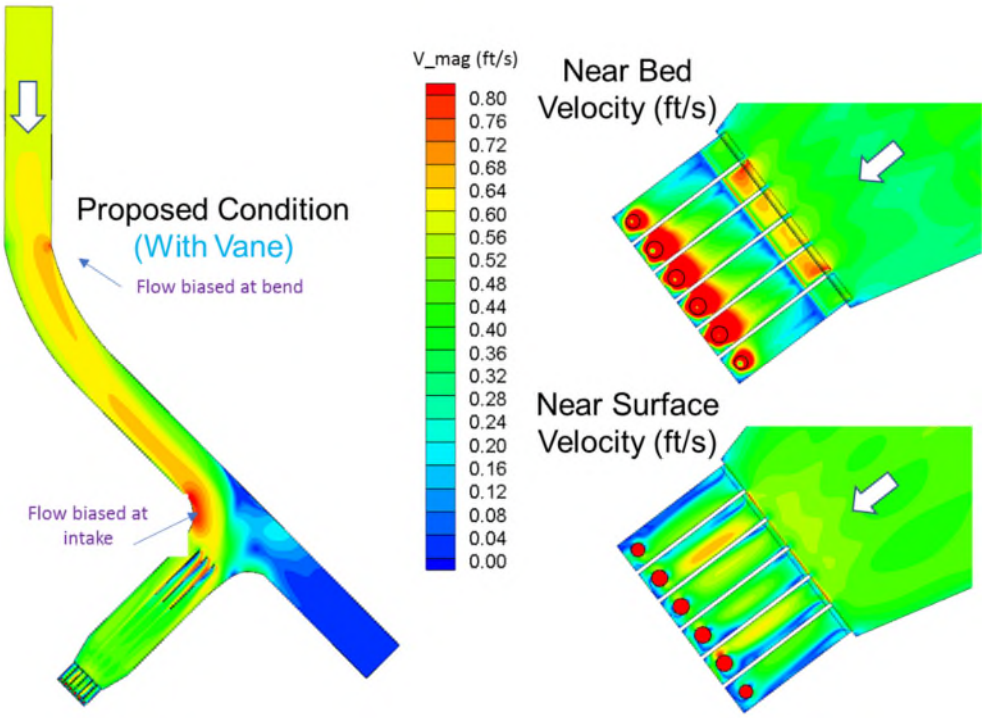

Figure 15. Flow field for the proposed design conditions at S332B with vanes, Scenario 1

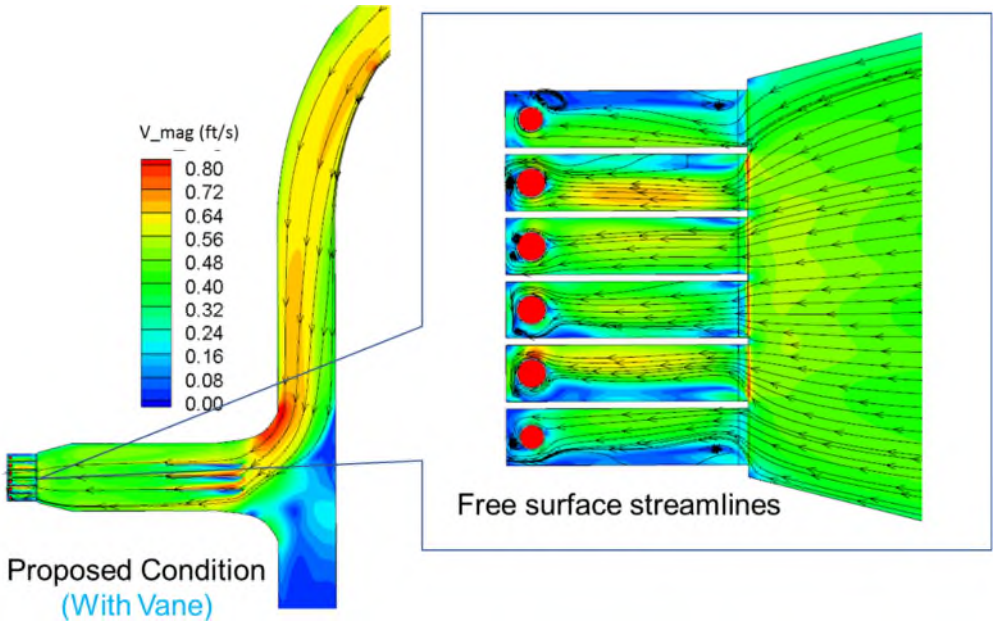

Figure 16. Streamlines for the proposed design conditions at S332B with vanes, Scenario 1

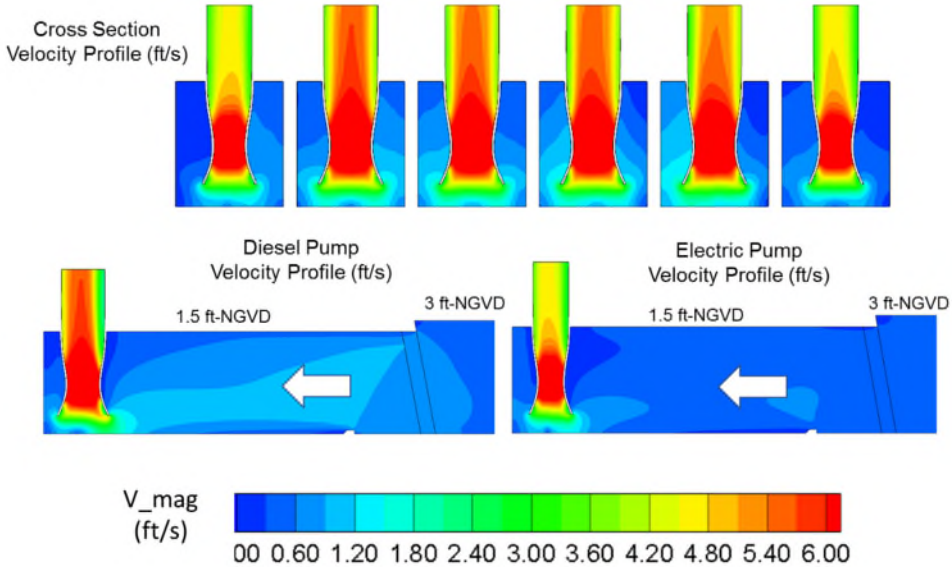

Figure 17. Cross-sectional velocity profiles for the proposed design conditions at S332B with vanes, Scenario 1

The forebay flow velocities approaching the pump bell were 1.4 ft/s at the diesel pumps, and 0.6 ft/s at the electric pumps. Since the diesel pumps have higher capacities, the velocities of the vortices within the barrels of these pumps were higher (5.5 ft/s). A vortex visualization using

3D streamlines for the proposed design condition with vanes is shown in Figure 18. The sub-surface vortices are clearly evident in this figure. Figure 19 shows the axial velocity distribution for the proposed design conditions with vanes. The figure confirms that the velocity distribution within the pump bell are centered at the origin.

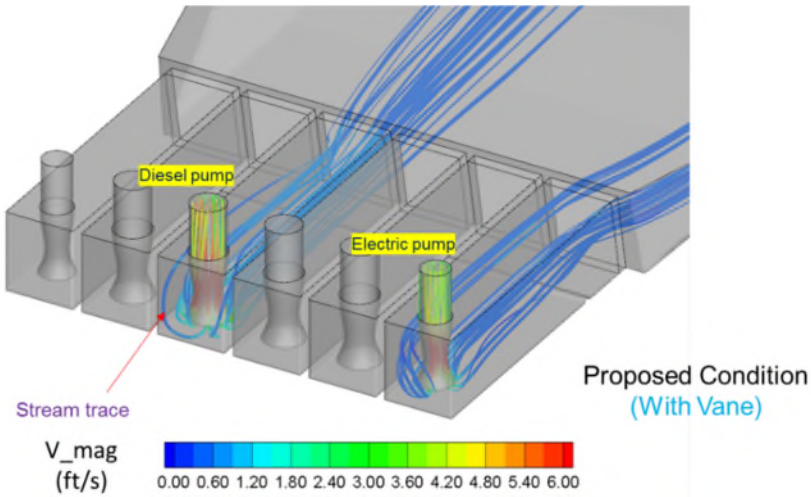

Figure 18. Vortex Visualization of the proposed design conditions at S332B with vanes, Scenario 1

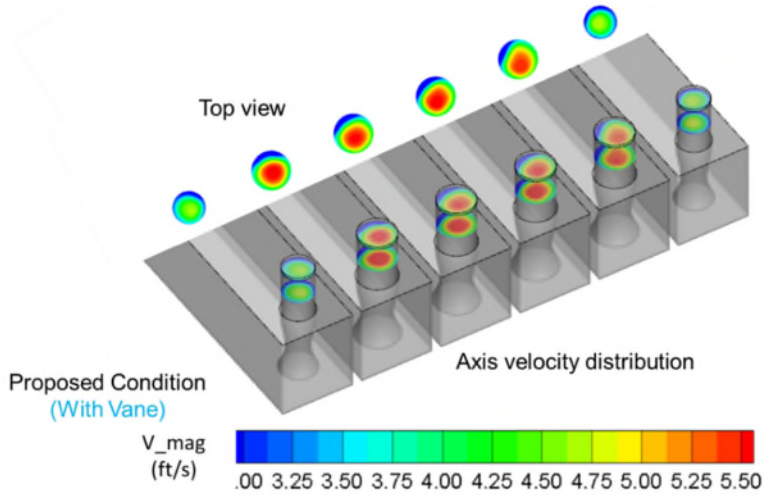

Figure 19. Axial velocity distribution for the proposed design conditions at S332B with vanes, Scenario 1

Model Simulations with a Trash Rack

Figure 20 through Figure 25 shows the results of the simulations of proposed design conditions at S332B with both a trash rack and flow separating vanes. With the vanes, the free surface velocities upstream of the pump station are close to 0.60 ft/s, while downstream in L-31N

canal they are less than 0.10 ft/s. The flow bias near the pump intakes is less for this scenario, as is evident in Figure 20. Additionally, the approach flow patterns at the pump intake are even (Figure 21).

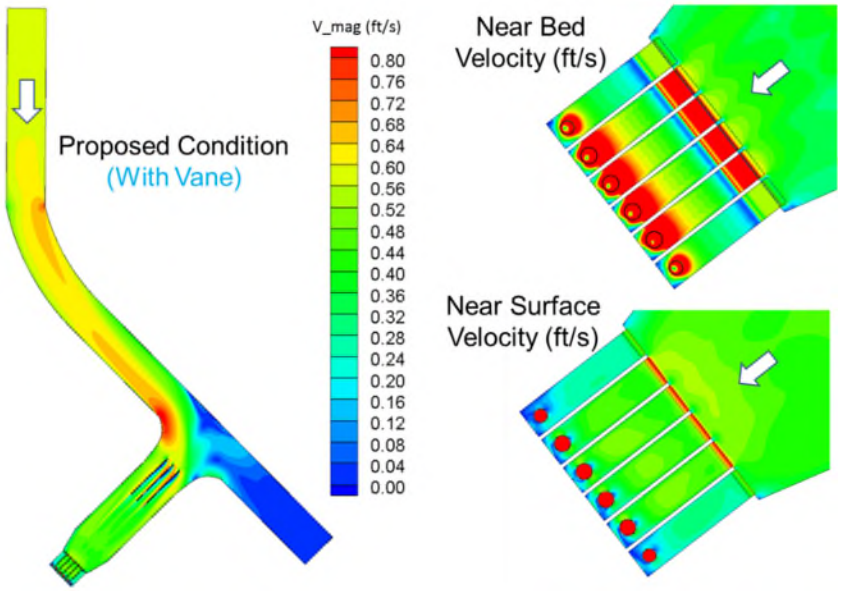

Figure 20. Flow field for the proposed design conditions at S332B with vanes and a trash rack, Scenario 1

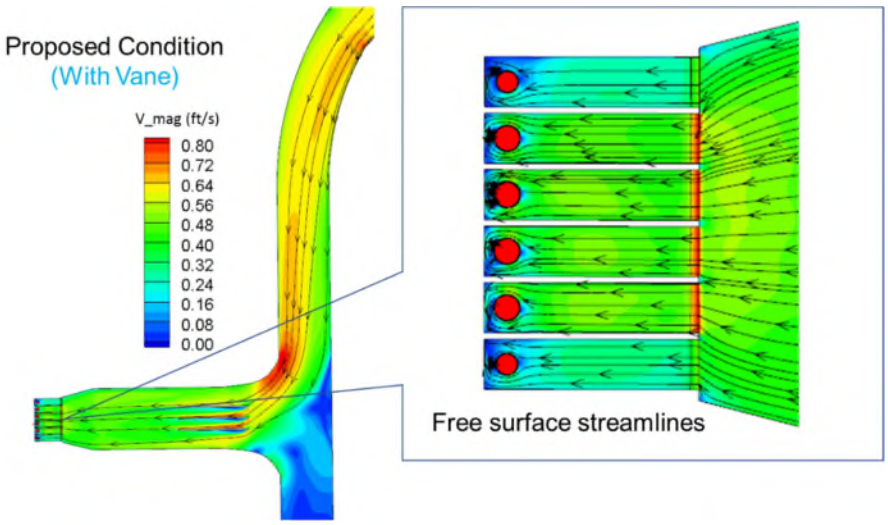

Figure 21. Streamlines for the proposed design conditions at S332B with vanes and a trash rack, Scenario 1

The cross-section velocity profiles in Figure 22 for the proposed design conditions with the trash rack and flow separating vanes illustrate an even flow distribution. As before, the relatively higher velocities at the diesel pumps are dues to their higher discharges. Sectional velocity profiles at the center of the pump configuration (Figure 23), indicate that the flow vortices

within the pump barrels are centered at their origins. Furthermore, the forebay flow velocities approaching the pump bells were 0.80 ft/s for the diesel pumps and 0.5 ft/s for the electric pumps. The velocities of the vortices within the barrels of these pumps were about 5.5 ft/s.

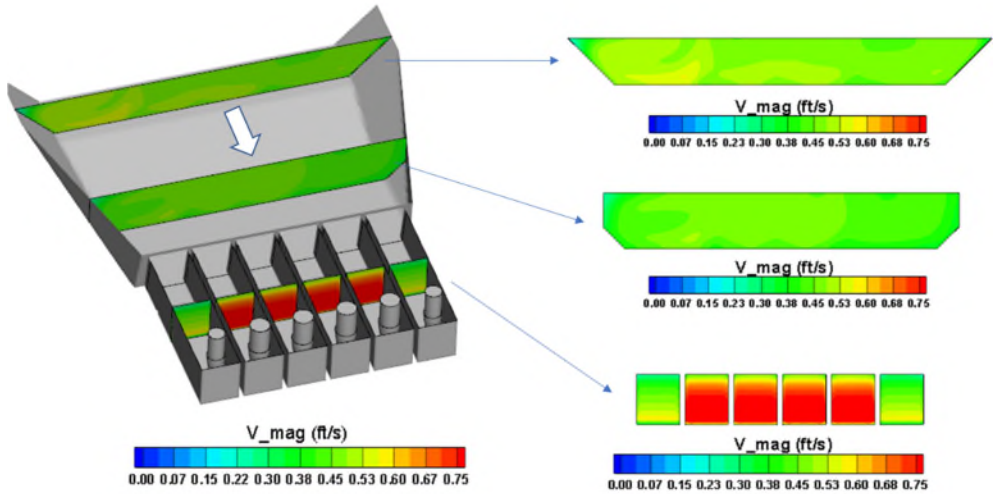

Figure 22. Cross-sectional velocity contours in the approaching canal and in the pump intakes for the S332B proposed design conditions with vanes and a trash rack (looking downstream), Scenario 1

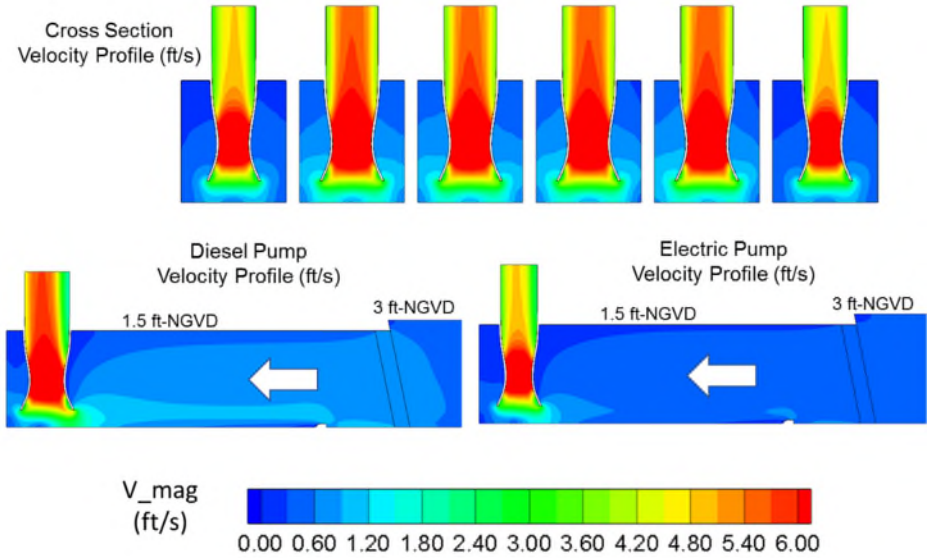

Figure 23. Cross-sectional velocity profiles for the S332B proposed design condition with vanes and a trash rack, Scenario 1

A 3-D vortex visualization for the proposed design conditions with the trash rack and flow separating vanes is shown in Figure 24. Figure 25 shows the corresponding axial velocity

distribution. It is evident that the velocity distribution within each pump suction bell is centered at the origin.

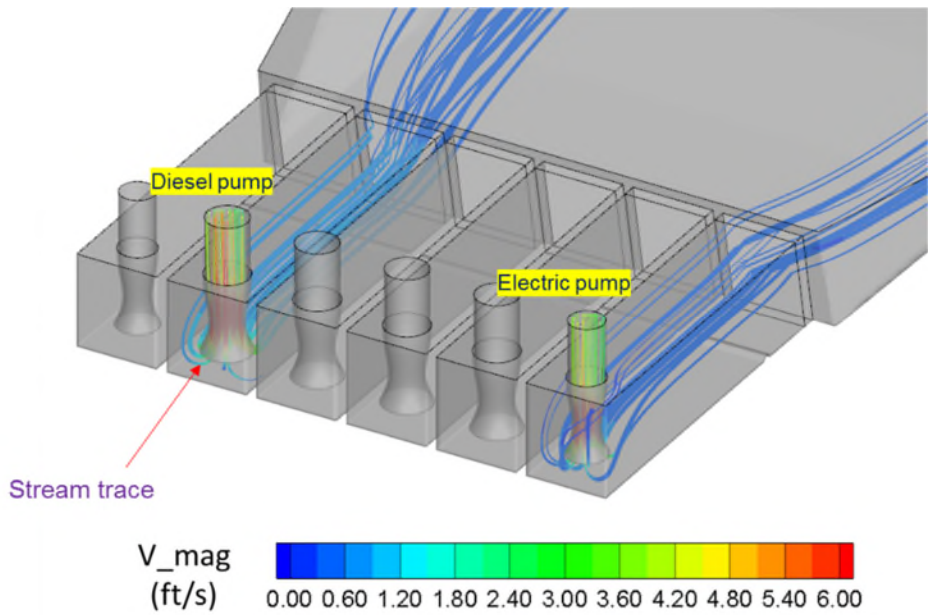

Figure 24. Vortex visualization with 3D streamlines for the S332B proposed design conditions with vanes and a trash rack, Scenario 1

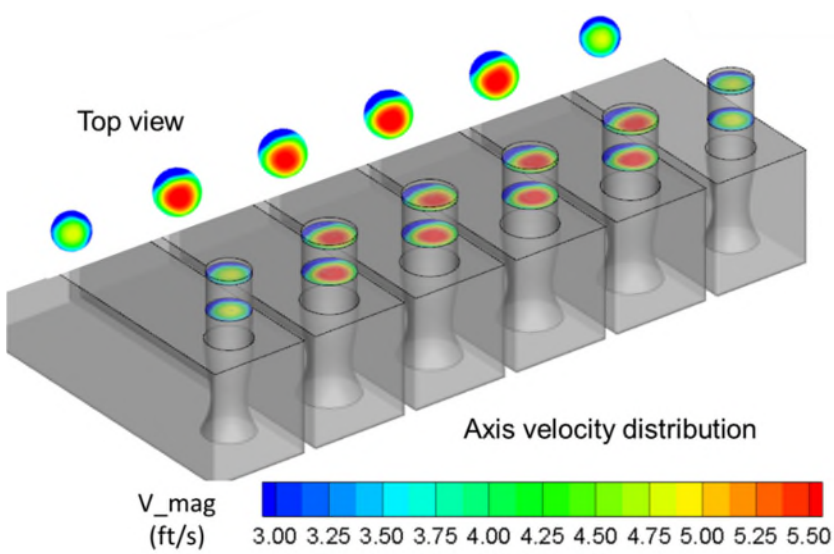

Figure 25. Axial velocity distribution for the S332B proposed design conditions with vanes and a trash rack, Scenario 1

S332C Existing Condition

The simulation of the flow fields within the approach canal, the forebays, and pump intakes

for the existing condition at S332C was conducted first to understand the deficiencies in the current design. The existing S332C pump layout contains four diesel units (125 cfs each), and one electric unit (75 cfs) placed in the middle. The CFD simulation was conducted with existing pump station operated at full capacity (575 cfs).

Figure 26 through Figure 31 show the simulation results for the existing conditions at the S332C pump station. Free surface velocities in the inflow canal upstream of the pump station are in the range of 0.5-0.6 ft/s while downstream of the pump station free surface velocities are less than 0.10 ft/s. A bias in the approach flow pattern is evident near the pump intakes as seen from the near-bed and near-surface velocity fields in Figure 26. The unbalanced flow distribution among the pump intakes can result in reduced hydraulic efficiencies and cause potential vibration issues.

Figure 27 shows the streamlines at the S332C pump station under existing conditions. The approaching flow is biased towards the right bank of the L-31N canal before it reaches the pump intakes and, close to the intakes, it keeps towards the right bank of the channel. A potential eddy formation is observed on the right bank of the canal near the channel bend.

The cross-section velocity profiles in Figure 28 under existing conditions at S332C also illustrate the biases in the approaching flows. Additionally, sectional velocity profiles along the centers of the pumps (Figure 29) reveal that the flow vortex within each pump intake is centered at the origin.

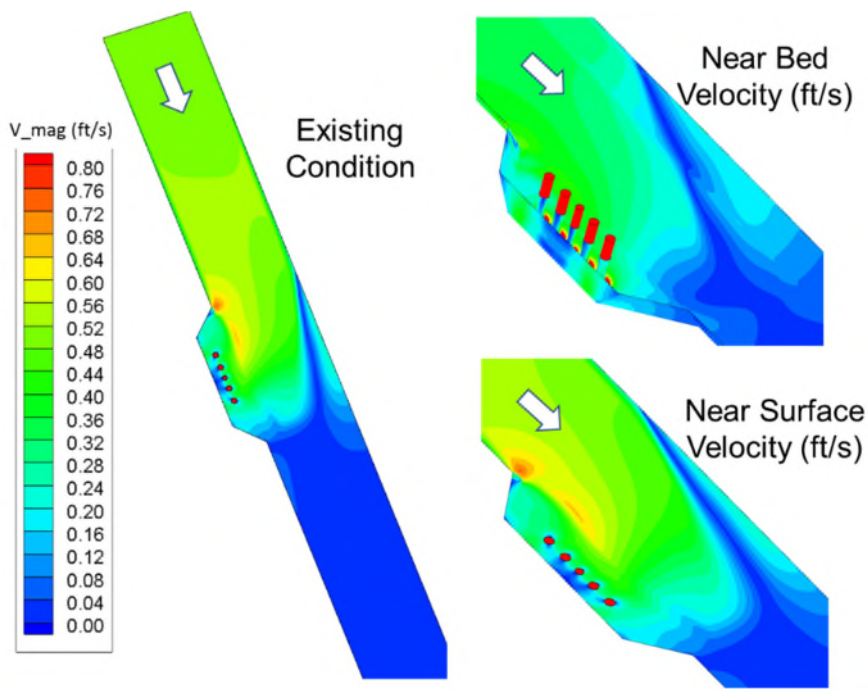

Figure 26. Flow field for existing condition at S332C

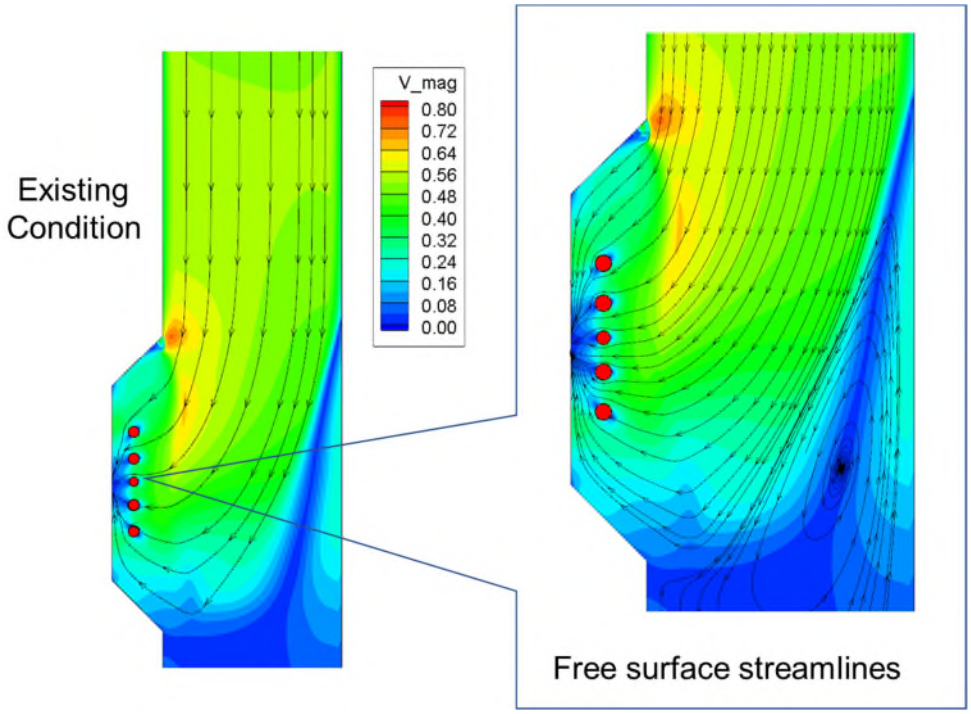

Figure 27. Flow lines, existing condition at S332C

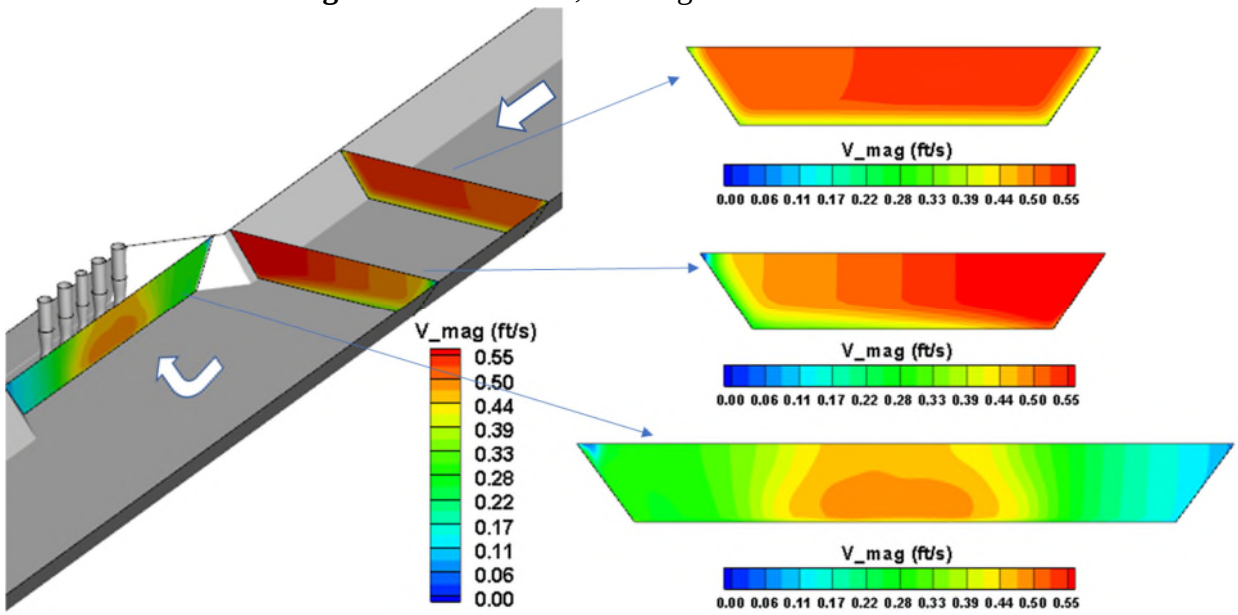

Figure 28. Cross-sections flow contours in approaching canal and in pump intakes, S332C existing condition (cross-sections are oriented looking downstream)

The flow velocities approaching the pump bell were about 0.60 ft/s at both the diesel and electric pumps. Since the diesel pumps have higher capacities, the velocities of the vortices within the intakes of these pumps were higher (5-6 ft/s). A visualization of the vortices for the existing conditions at S332C using 3D streamlines is shown in Figure 30.

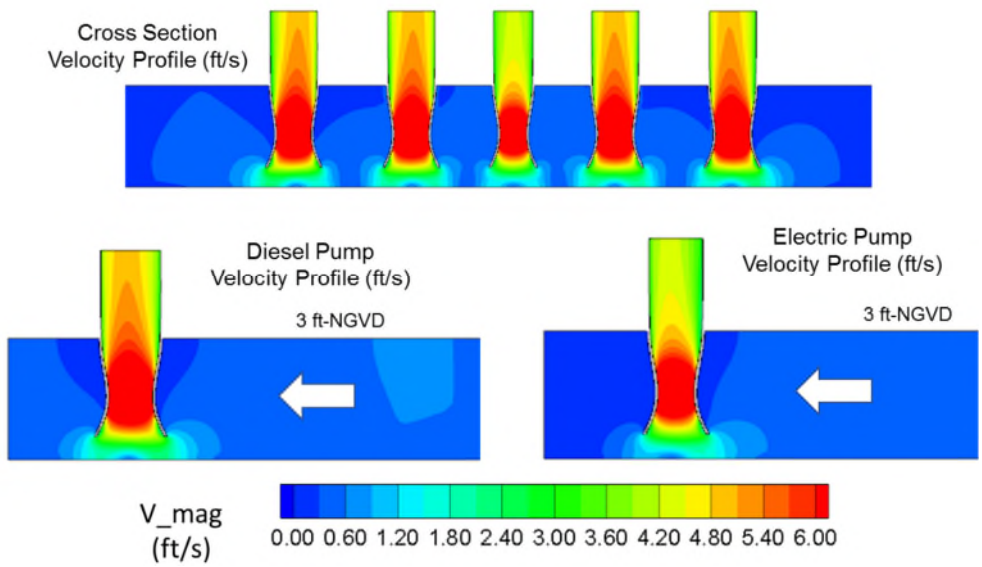

Figure 29. Cross-section velocity profiles, S332C existing condition

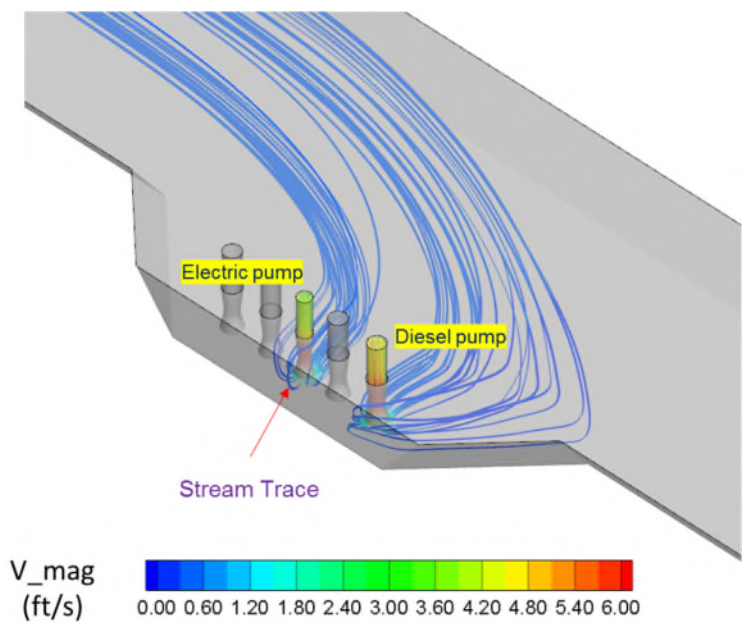

Figure 30. Visualization of vortex using 3D streamlines, S332C existing condition

Figure 31 shows the axial velocity distribution within each pump intake under existing conditions at S332C. The figure shows that the velocity distribution within each pump suction bell is approximately centered at the origin, a confirmation of Figure 29.

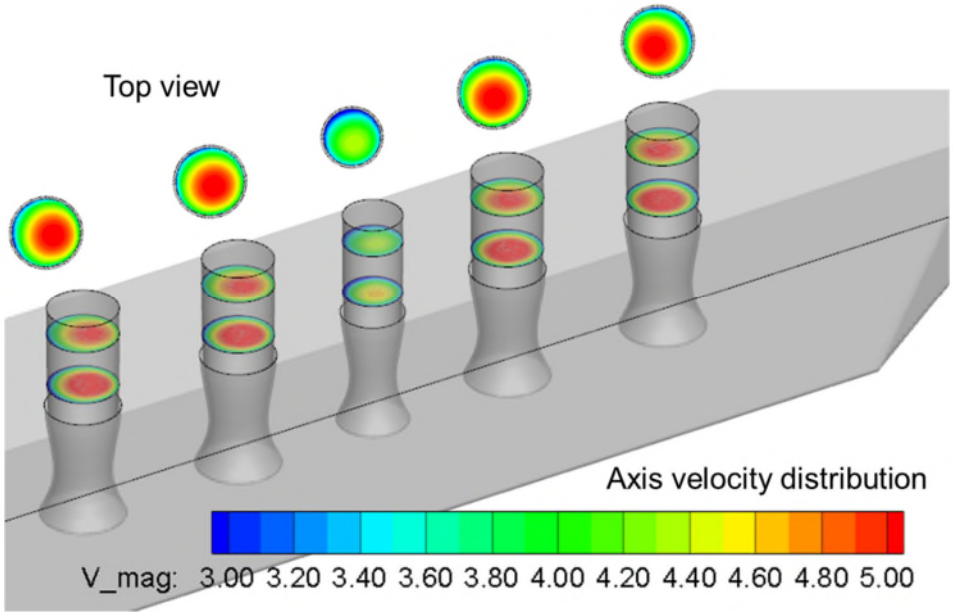

Figure 31. Axis velocity distribution, S332C existing condition

S332C Proposed Condition

Two set of model simulations were conducted for S332C pump station with the proposed condition, (i) without trash rack, and (ii) with trash rack. Each simulation is discussed below separately. For the proposed condition, the full pump capacity is 650 cfs.

Model Simulations Without a Trash Rack

Figure 32 through Figure 37 show the results of the simulations for the proposed conditions without the trash rack. Two different simulations were conducted for this scenario, (i) without vanes, and (ii) with vanes. Without vanes, the free surface velocities upstream of the pump station are close to 0.60 ft/s while at downstream in L-31N canal is less than 0.10 ft/s. Potentials of eddy formation near the channel bend is observed for this scenario, and the approaching flow is biased towards the left bank. This leads to an uneven approach flow pattern at the pumps. The incorporation of vanes into the design resolved this problem, as is evident in Figure 33. The flow bias reduces due to the vanes, and discharge is directed evenly towards the pump intake. The improvement in the flow distribution can be seen from the near surface velocity field.

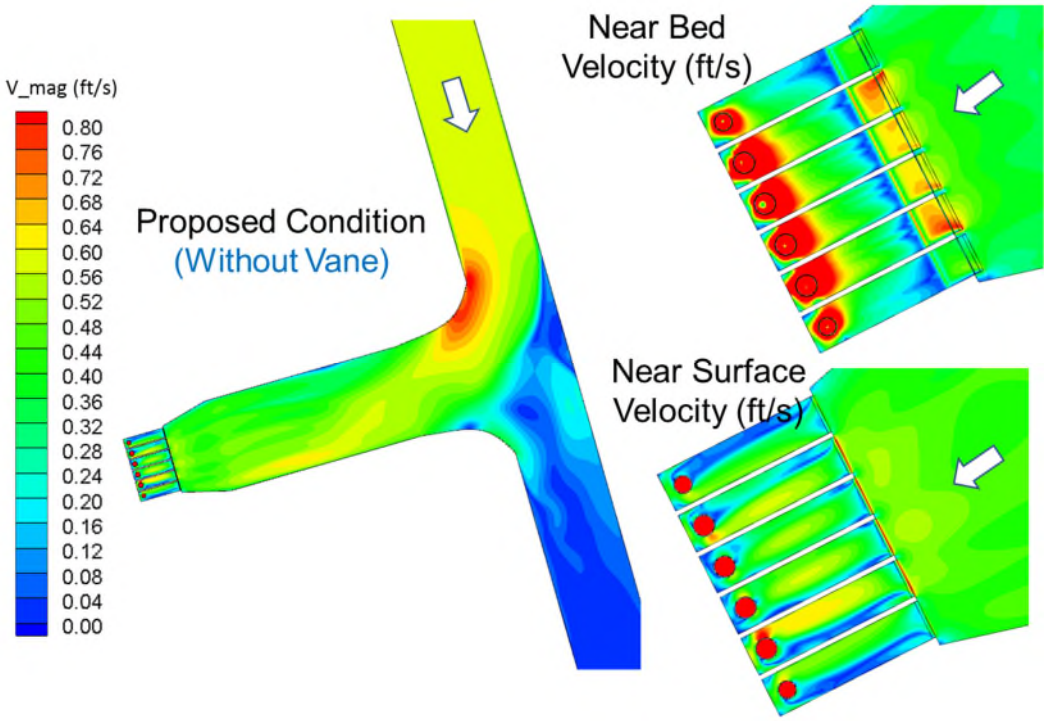

Figure 32. Flow field for the proposed design conditions at S332C without vanes, Scenario 1

Figure 34 shows the streamlines approaching S332C under the proposed conditions with vanes. It is also evident that forebay flows approaching the pump bells are even. These unbiased flow distributions should help attain higher hydraulic pump efficiencies.

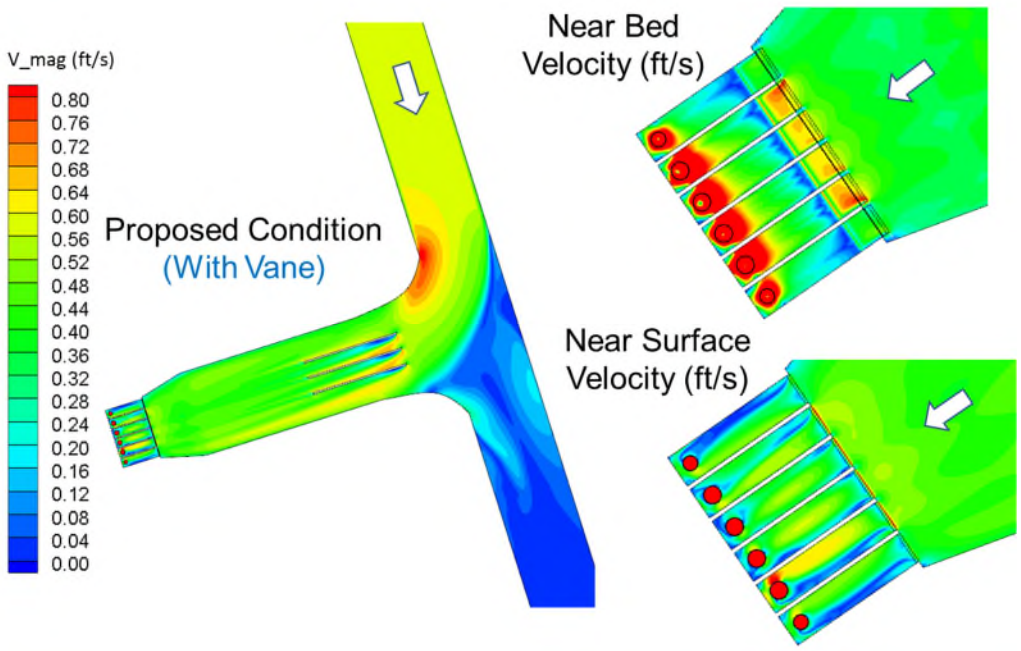

Figure 33. Flow field for the proposed design conditions at S332C with vanes, Scenario 1

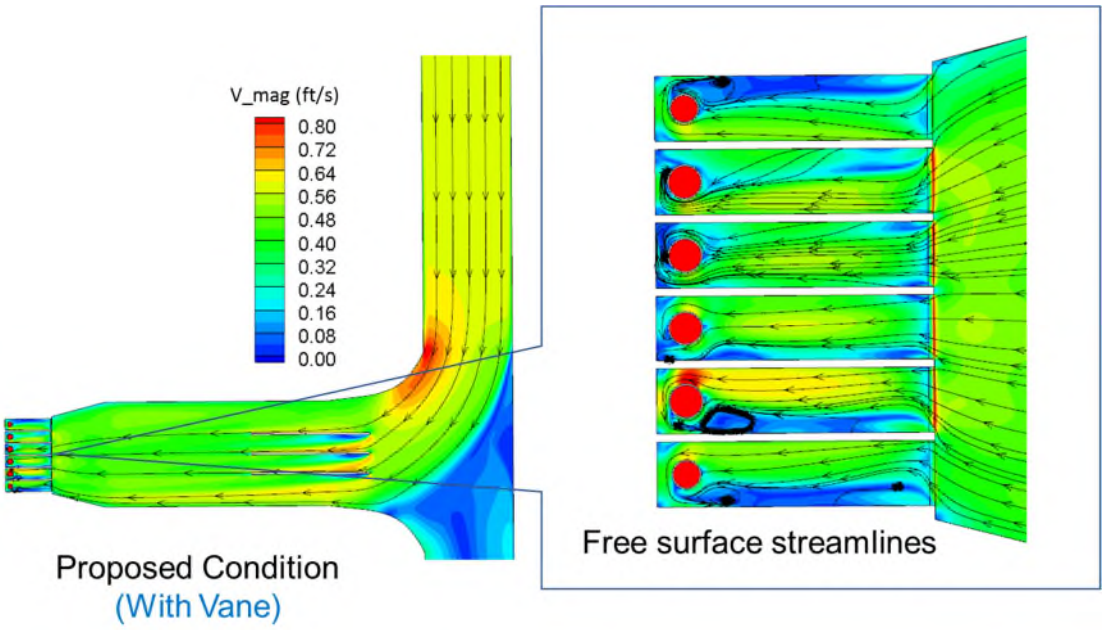

Figure 34. Streamlines for the proposed design conditions at S332C with vanes, Scenario 1

The cross-section velocity profiles for the proposed design conditions with the flow separating vanes are shown in Figure 35. The forebay flow velocities approaching the pump bell

were 1.2 ft/s at the diesel pumps, and 0.5 ft/s at the electric pumps. Since the diesel pumps have higher capacities, the velocities of the vortices within the barrels of these pumps were higher.

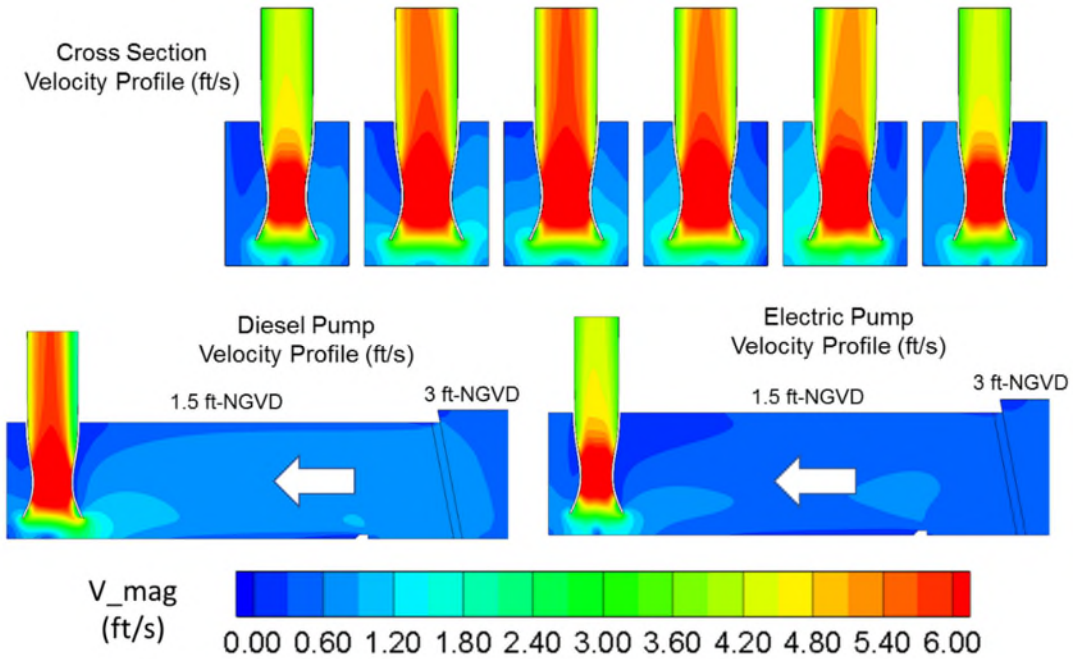

Figure 35. Cross-sectional velocity profiles for the proposed design conditions at S332C with vanes, Scenario 1

A vortex visualization using 3D streamlines for the proposed design condition with vanes is shown in Figure 36. The sub-surface vortices are clearly evident in this figure. Figure 37 shows the axial velocity distribution for the proposed design conditions at with vanes. Figure 37 confirms that the velocity distribution within each pump bell is centered at the origin.

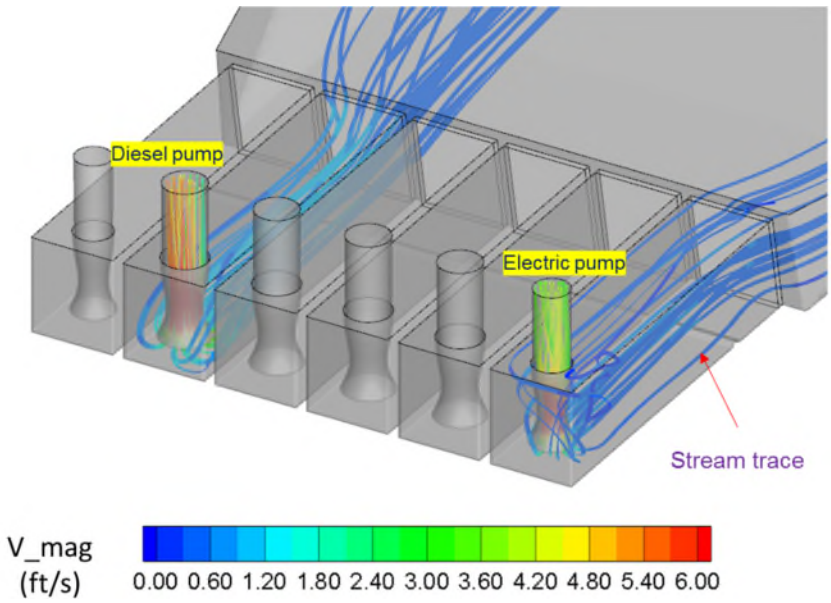

Figure 36. Vortex Visualization of the proposed design conditions at S332C with vanes, Scenario 1

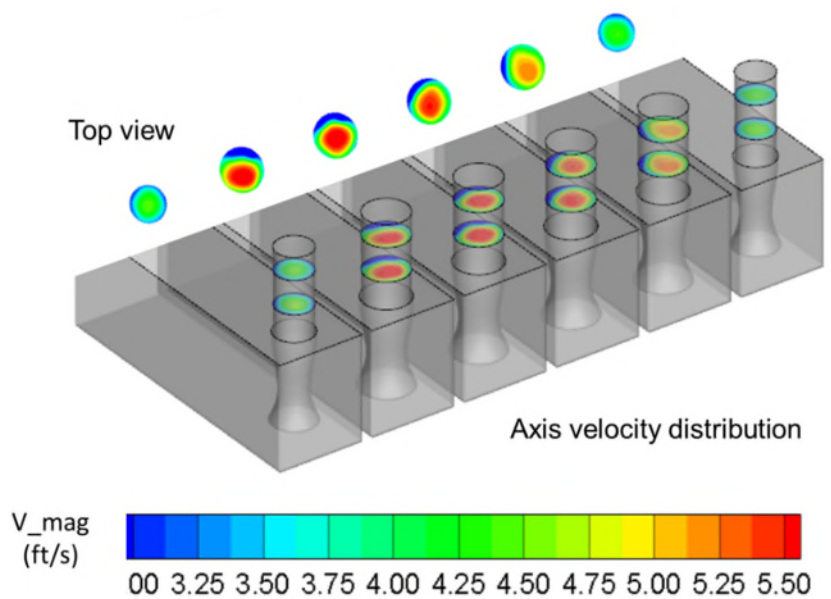

Figure 37. Axial velocity distribution for the proposed design conditions at S332C with vanes, Scenario 1

Model Simulations with a Trash Rack

Figure 38 through Figure 43 show the results of the simulations of proposed design conditions at S332B with both trash rack and flow separating vanes. With the trash rack and vanes, the free surface velocities upstream of the pump station are close to 0.60 ft/s, while downstream

in L-31N canal they are less than 0.10 ft/s. The flow bias near the pump intakes is less for this scenario, as is evident in Figure 38. Additionally, the approach flow patterns at the pump intake are even. These unbiased flow distributions should help attain higher hydraulic pump efficiencies and reduce vibration issues. Figure 39 shows the streamlines approaching S332C under proposed conditions with vanes and trash rack. The improvement in the flow distribution can be seen from the near surface velocity field.

The cross-section velocity profiles in Figure 40 for the proposed design conditions with the trash rack and flow separating vanes illustrate an even flow distribution. As before, the relatively higher velocities at the diesel pumps are dues to their higher discharges. Sectional velocity profiles at the center of the pump configuration (Figure 41) indicate that the flow vortices within the pump barrels are centered at their origins. Furthermore, the forebay flow velocities approaching the pump bells were 1.0 ft/s for the diesel pumps and 0.4 ft/s for the electric pumps. The velocities of the vortices within the barrels of these pumps were about 5.5 ft/s.

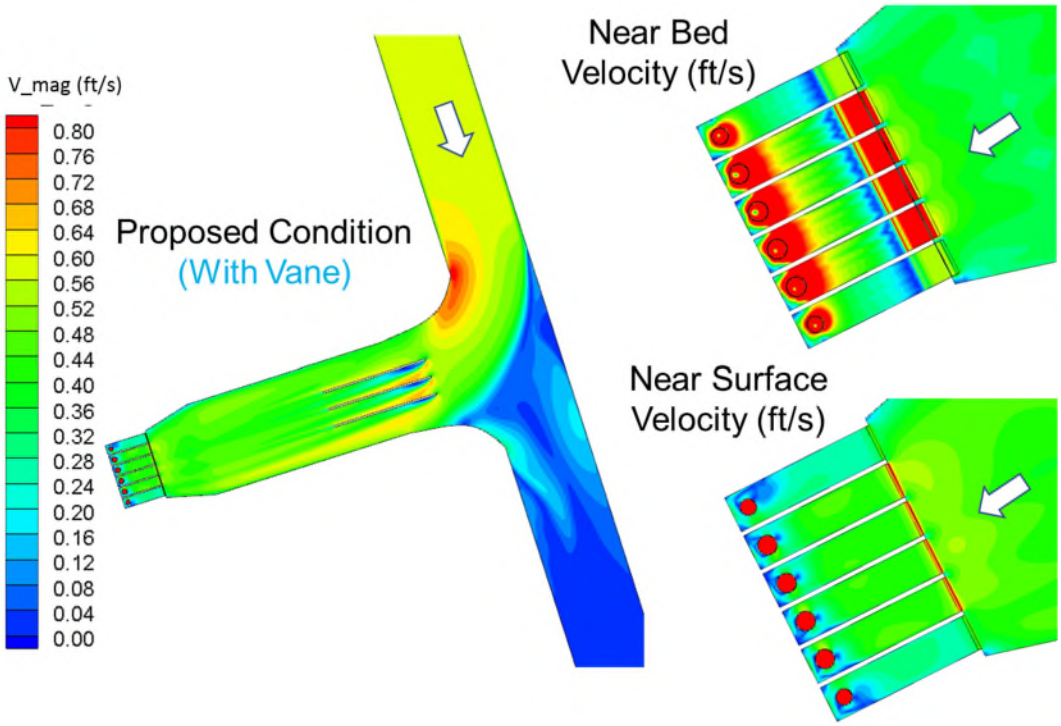

Figure 38. Flow field for the proposed design conditions at S332C with vanes and a trash rack, Scenario 1

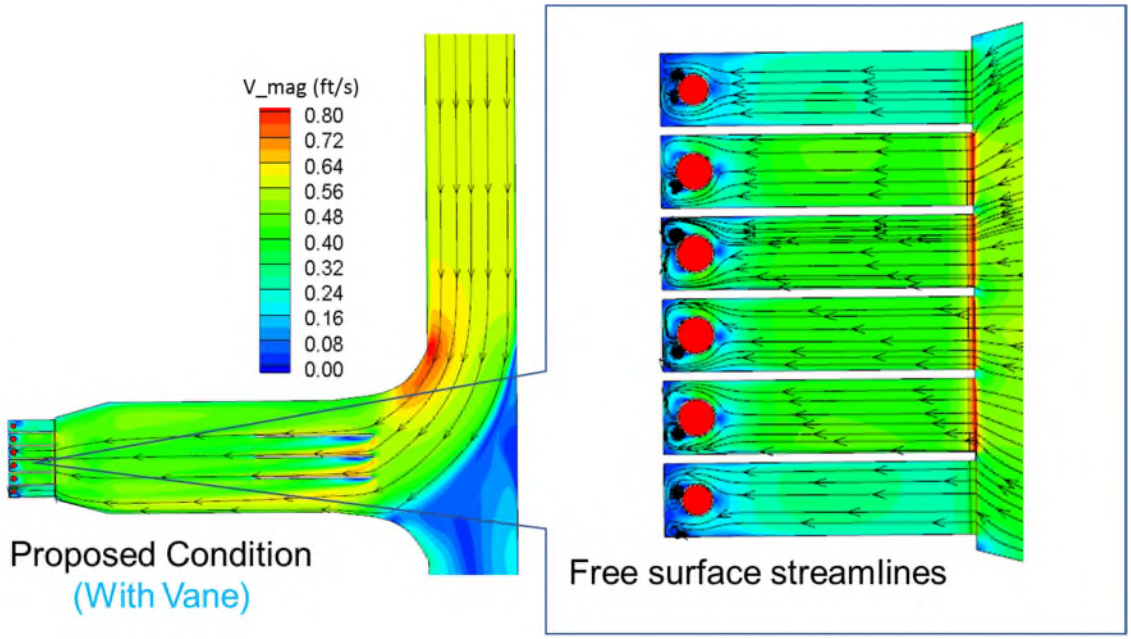

Figure 39. Streamlines for the proposed design conditions at S332C with vanes and a trash rack, Scenario 1

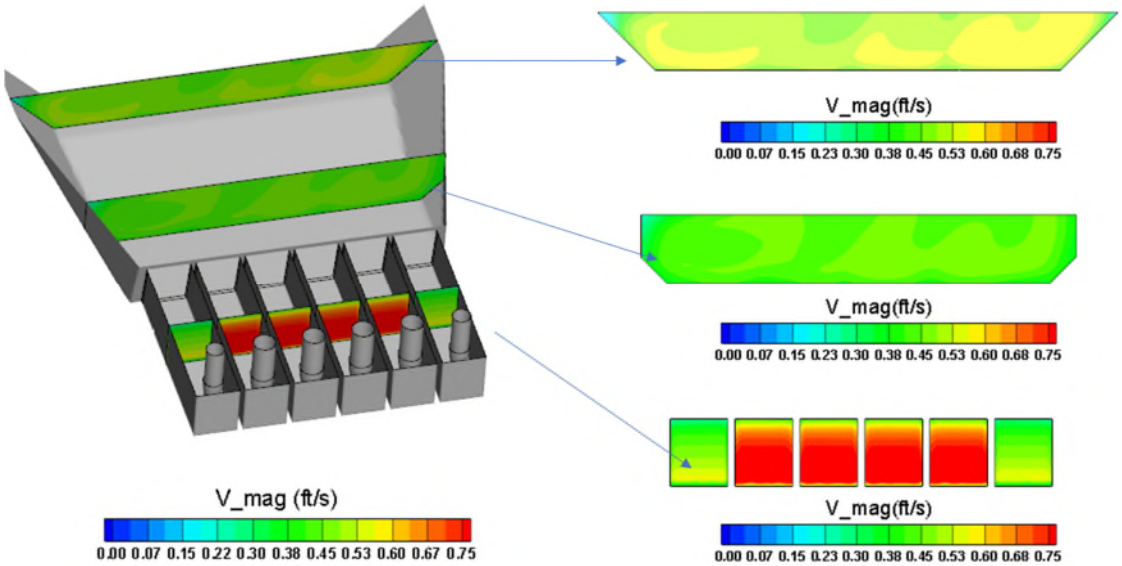

Figure 40. Cross-sectional velocity contours in the approaching canal and in the pump intakes for the S332C proposed design conditions with vanes and a trash rack (cross-sections are oriented looking downstream), Scenario 1

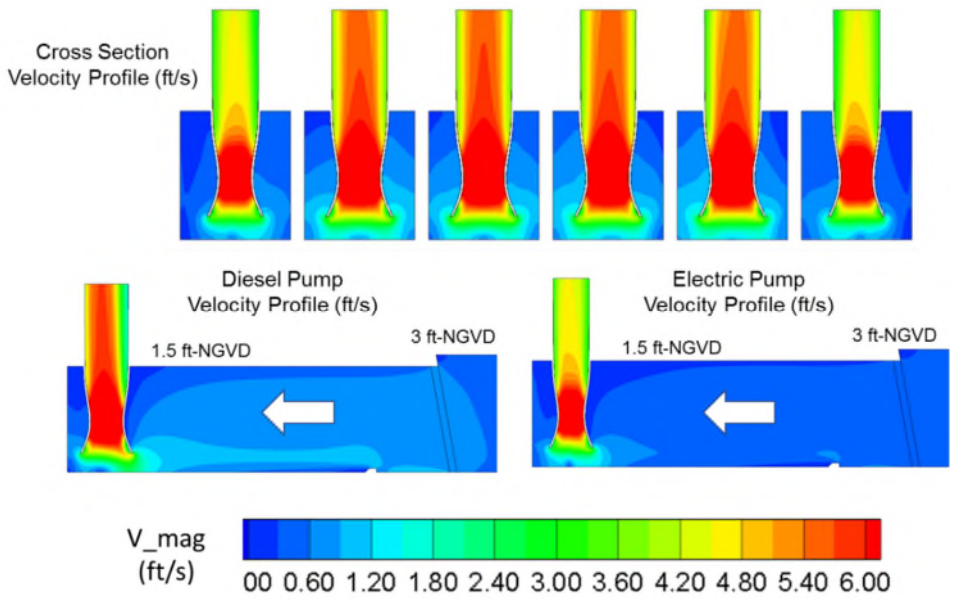

Figure 41. Cross-sectional velocity profiles for the S332C proposed design condition with vanes and a trash rack, Scenario 1

A 3-D vortex visualization for the proposed design conditions with the trash rack and flow separating vanes is shown in Figure 42. The sub-surface vortices can be observed from this figure. Figure 43 shows the corresponding axial velocity distribution. It is evident that the velocity distribution within each pump suction bell is centered at the origin, also seen from Figure 41.

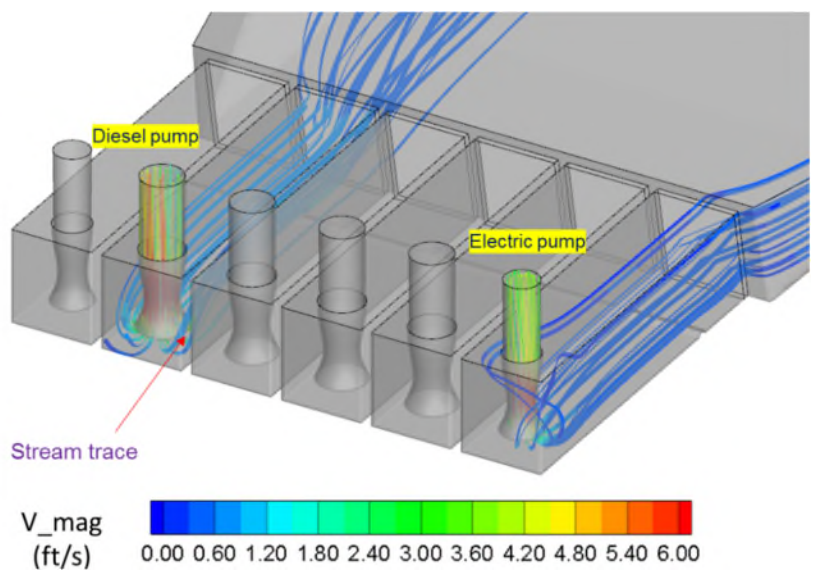

Figure 42. Vortex visualization with 3D streamlines for the S332C proposed design conditions with vanes and a trash rack, Scenario 1

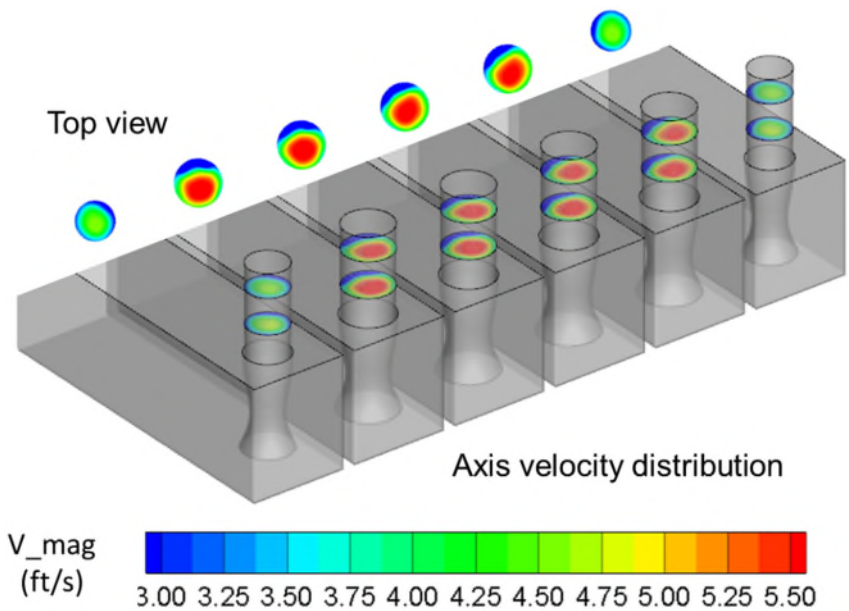

Figure 43. Axial velocity distribution for the proposed S332C design conditions with vanes and a trash rack, Scenario 1

SCENARIO 2

For both S332B and C, one electric pump unit (75 cfs) is designed as redundancy. This section presents the results of the CFD analyses for the operation scenario with one electric pump inactive at the S332B and S332C pump stations. For this scenario, the total pump capacity is 575 cfs. The recommended design with trash rack and flow separating vanes from Scenario 1 CFD simulations was considered for the analyses for this scenario.

S332B Proposed Condition

Simulation was conducted for the operation scenario evaluation, with trash rack. Figure 44 through Figure 49 show the results of the simulation of the scenario at S332B with both trash rack and flow separating vanes with pump capacity of 575 cfs. The free surface velocities upstream of the station are close to 0.60 ft/s, while downstream in L-31N canal they are less than 0.10 ft/s (Figure 44). The flow bias near the pump intakes is with the vanes, and discharge is directed evenly towards the pump intake. The flow distribution is similar to Scenario 1 with 650 cfs.

Figure 45 shows the streamlines approaching S332B under the proposed conditions with vanes. It is evident that forebay flows approaching the pump bells are even. This is also evident in the cross-section flow contours shown in Figure 46. The unbiased flow distributions should help attain higher hydraulic pump efficiencies.

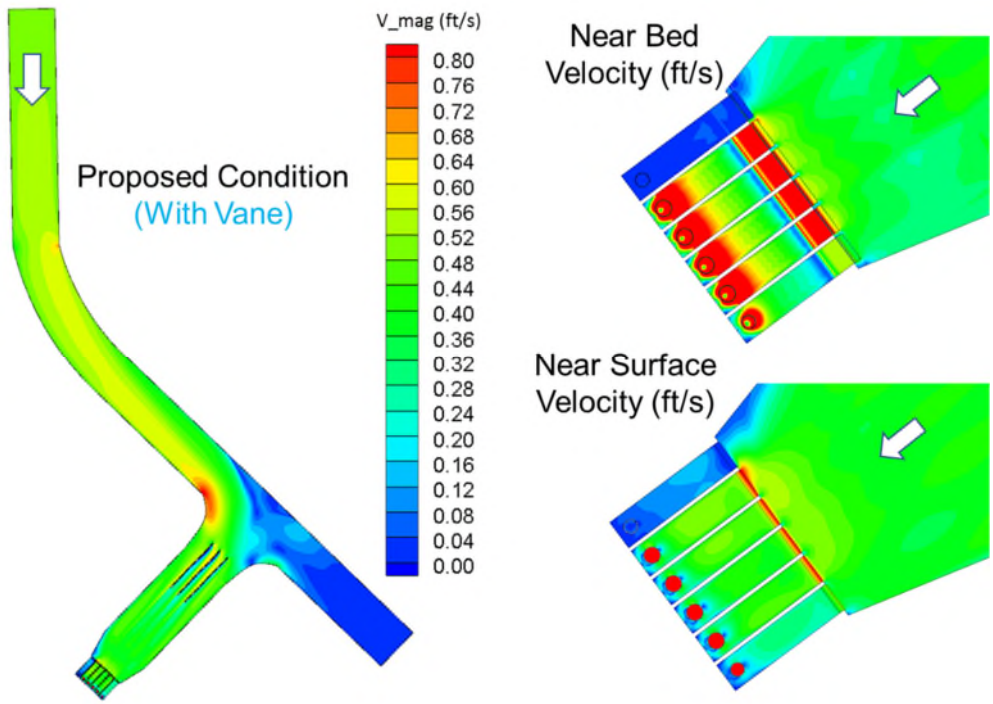

Figure 44. Flow field for the proposed design conditions at S332B with vanes, Scenario 2

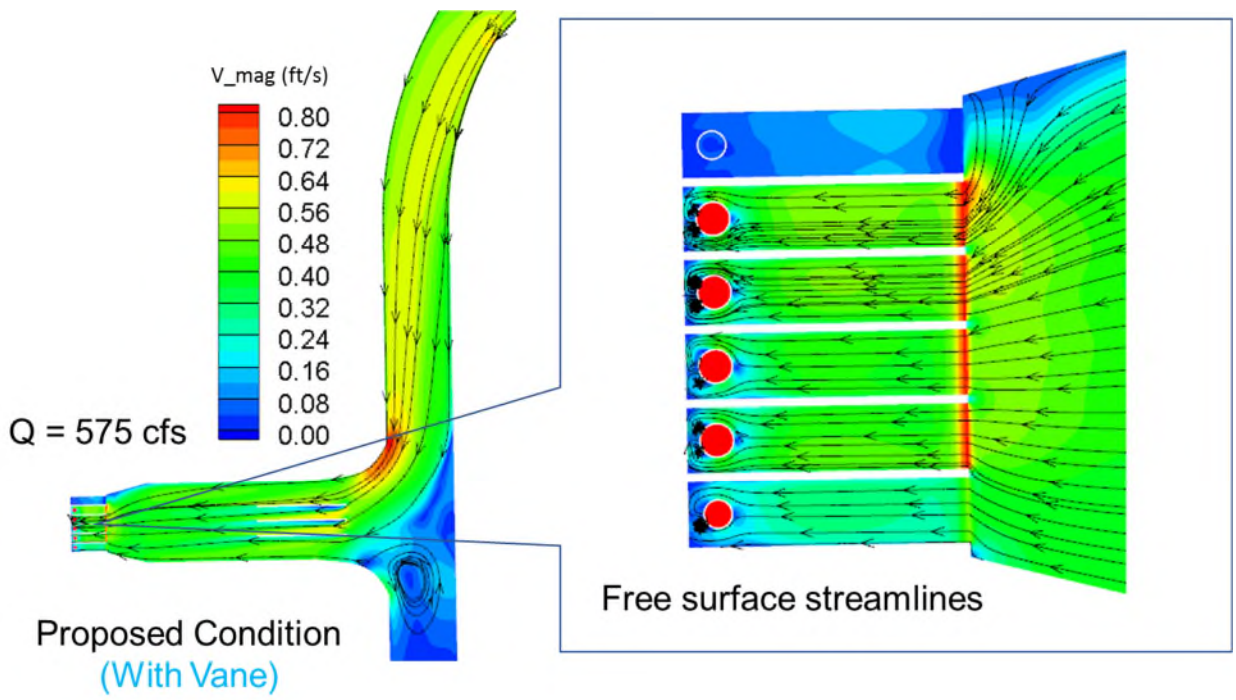

Figure 45. Streamlines for the proposed design conditions at S332B with vanes, Scenario 2

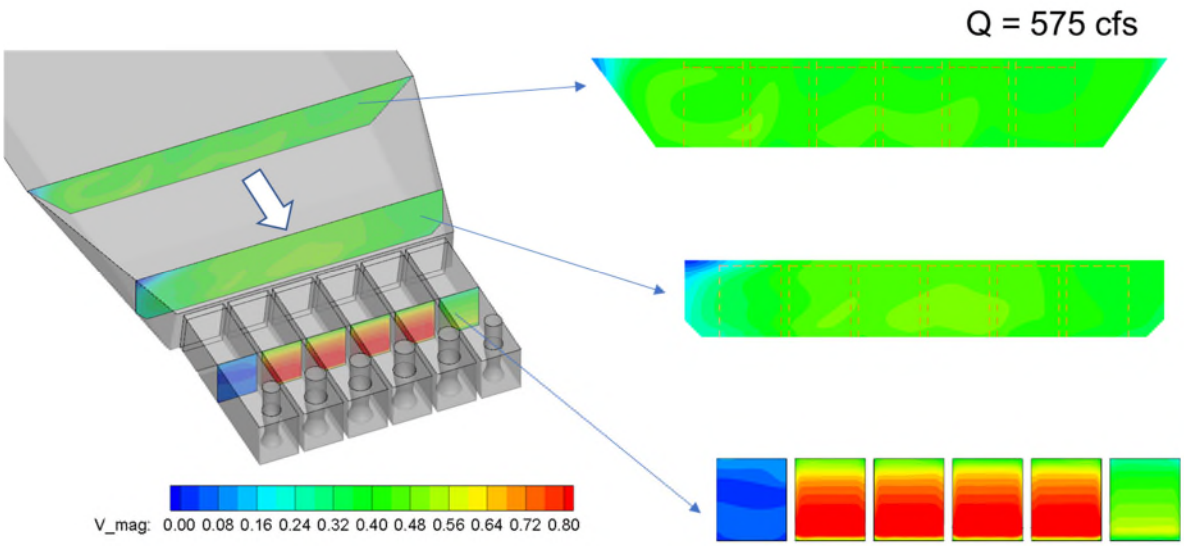

Figure 46. Cross-sectional velocity contours in the approaching canal and in the pump intakes for the S332B proposed design conditions with vanes and a trash rack (cross-sections are oriented looking downstream), Scenario 2

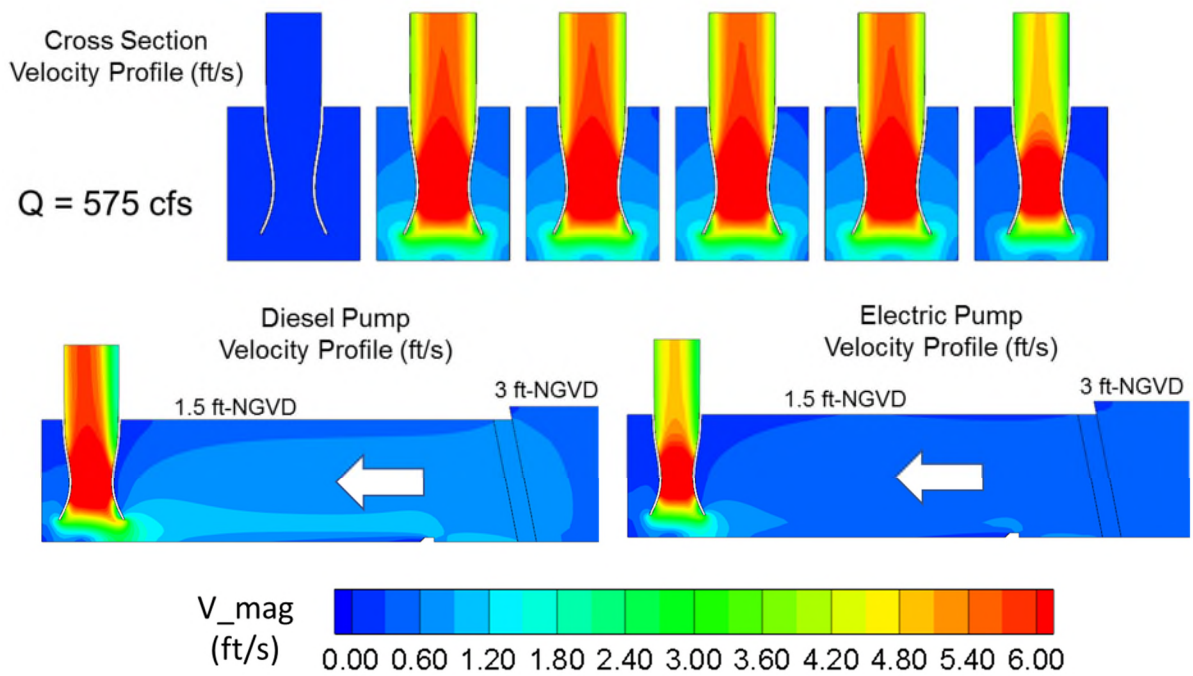

Figure 47. Cross-sectional velocity profiles for the proposed design conditions at S332B with vanes, Scenario 2

The cross-section velocity profiles in Figure 47 for the proposed condition with the trash rack and flow separating vanes illustrates that the flow distribution is even with the 575 cfs pump capacity. Since the diesel pumps have higher capacities, the velocities of the vortices within the barrels of these pumps were higher. Sectional velocity profiles at the center of the pump configuration indicate that the flow vortices within the pump barrels are centered at their origins. The forebay flow velocities approaching the pump bell were 0.80 ft/s at the diesel pumps, and 0.50 ft/s at the electric pumps. The flow distribution and velocities for Scenario 2 (575 cfs) are similar to Scenario 1 (650 cfs).

A vortex visualization using 3D streamlines for the proposed design condition with vanes and trash rack is shown in Figure 48. The sub-surface vortices are clearly evident in this figure. Figure 49 shows the axial velocity distribution for the proposed design conditions at with vanes. Figure 49 confirms that the velocity distribution within each pump bell is centered at the origin.

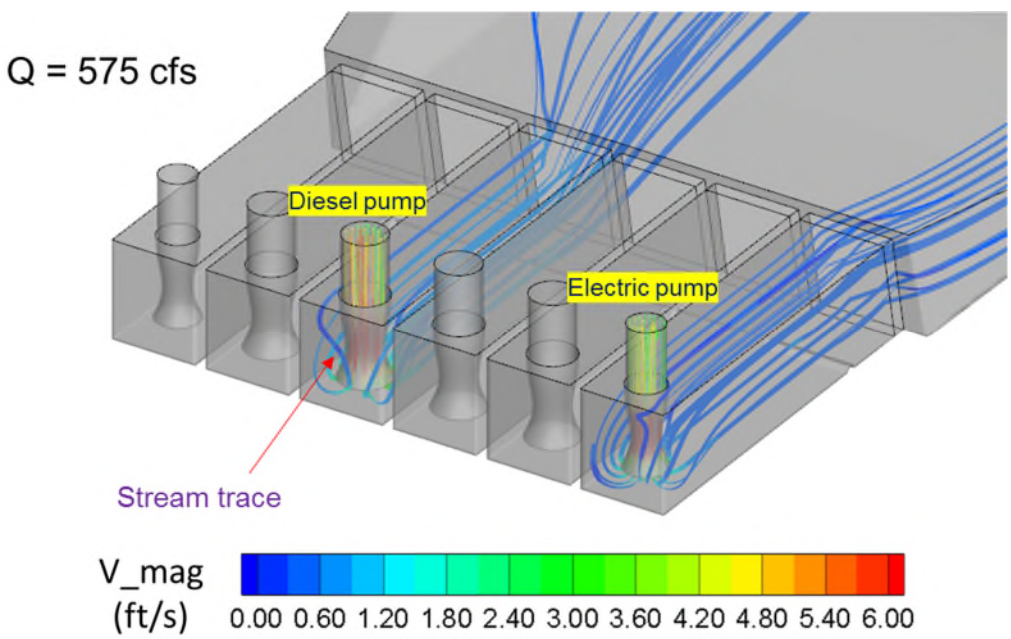

Figure 48. Vortex Visualization of the proposed design conditions at S332B with vanes, Scenario 2

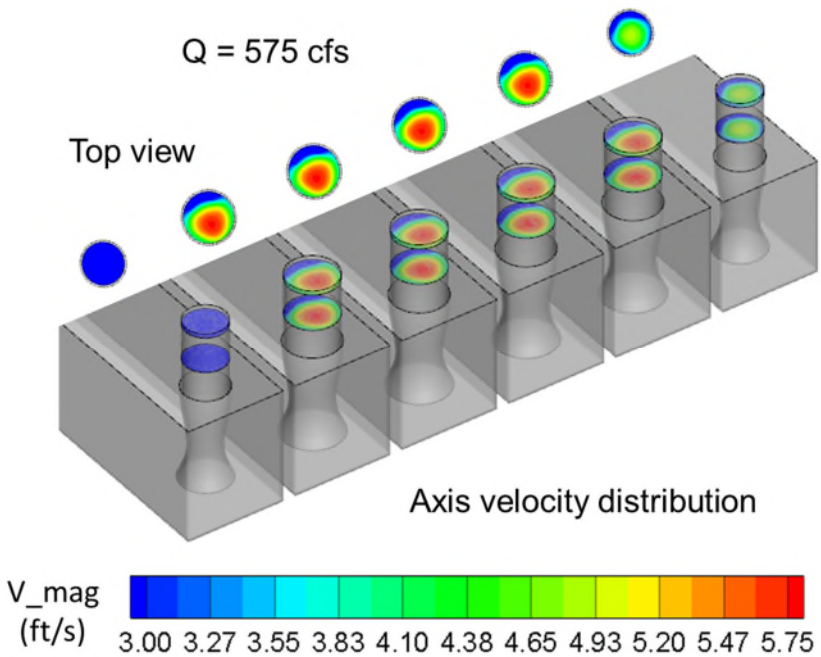

Figure 49. Axial velocity distribution for the proposed design conditions at S332B with vanes, Scenario 2

S332C Proposed Condition

Figure 50 through Figure 55 shows the results of the simulation for the proposed condition at S332C pump station without considering the trash rack and vanes for 575 cfs pump capacity. Free surface velocities upstream of the pump station are close to 0.60 ft/s, while downstream they are less than 0.10 ft/s. The flow bias near the pump intakes is less for this scenario. Additionally, the discharge is directed evenly towards the pump intake. The flow distribution seen from the near bed and near surface velocity fields are similar to those for Scenario 1 (650 cfs). Figure 51 shows the flow lines at the S332C pump station for the proposed condition with vanes. These unbiased flow distributions should help attain higher hydraulic pump efficiencies.

The unbiased flow distribution is also evident in the associated cross-section flow contours shown in Figure 52. As before, the relatively higher velocities at the diesel pumps are dues to their higher discharges. Sectional velocity profiles at the center of the pump configuration (Figure 53) indicate that the flow vortices within the pump barrels are centered at their origins. Furthermore, the forebay flow velocities approaching the pump bells were 1.0-1.2 ft/s for the diesel pumps and 0.4 ft/s for the electric pumps. The velocities of the vortices within the barrels of these pumps were about 5.5 ft/s.

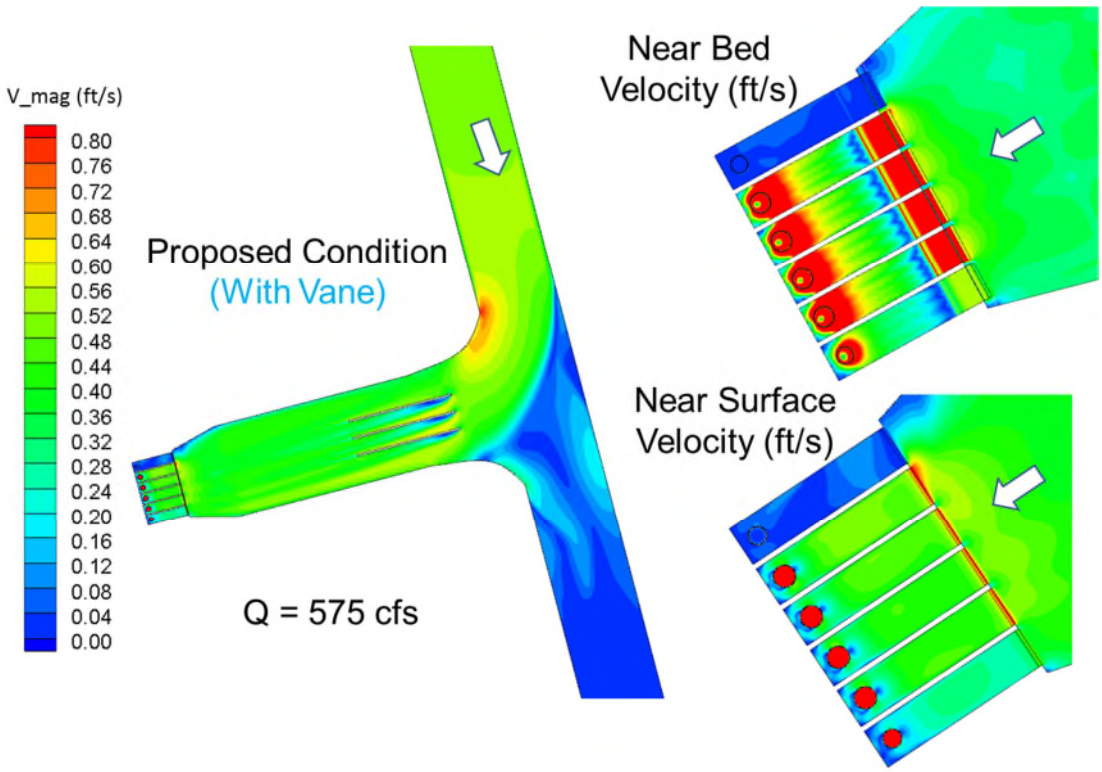

Figure 50. Flow field for the proposed design conditions at S332C with vanes and a trash rack, Scenario 2

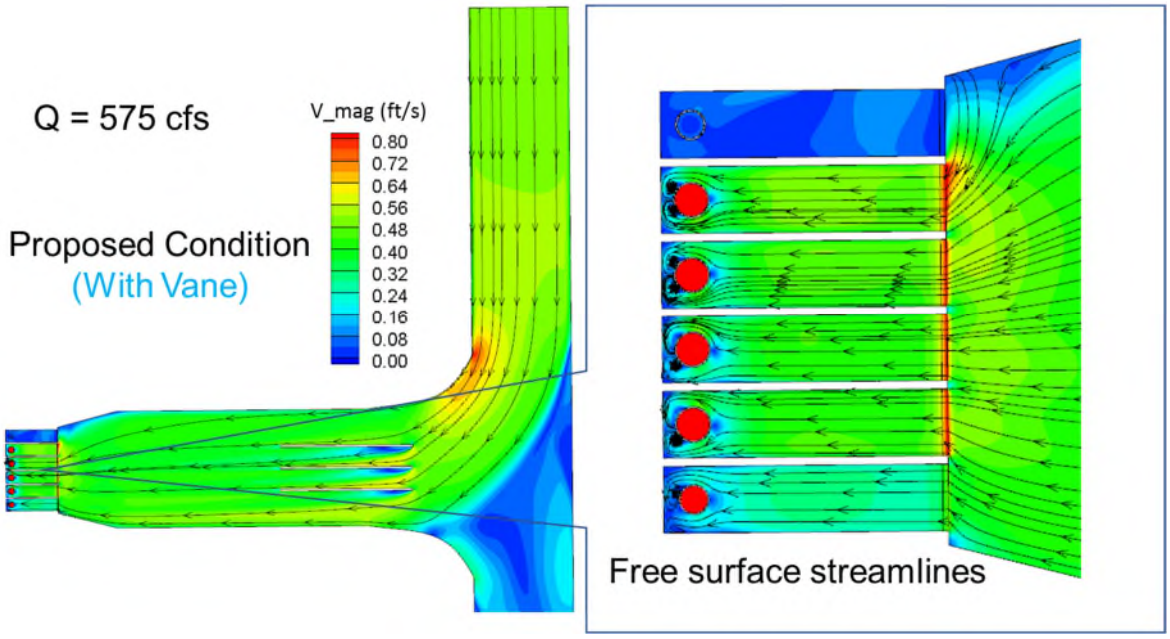

Figure 51. Streamlines for the proposed design conditions at S332C with vanes and a trash rack, Scenario 2

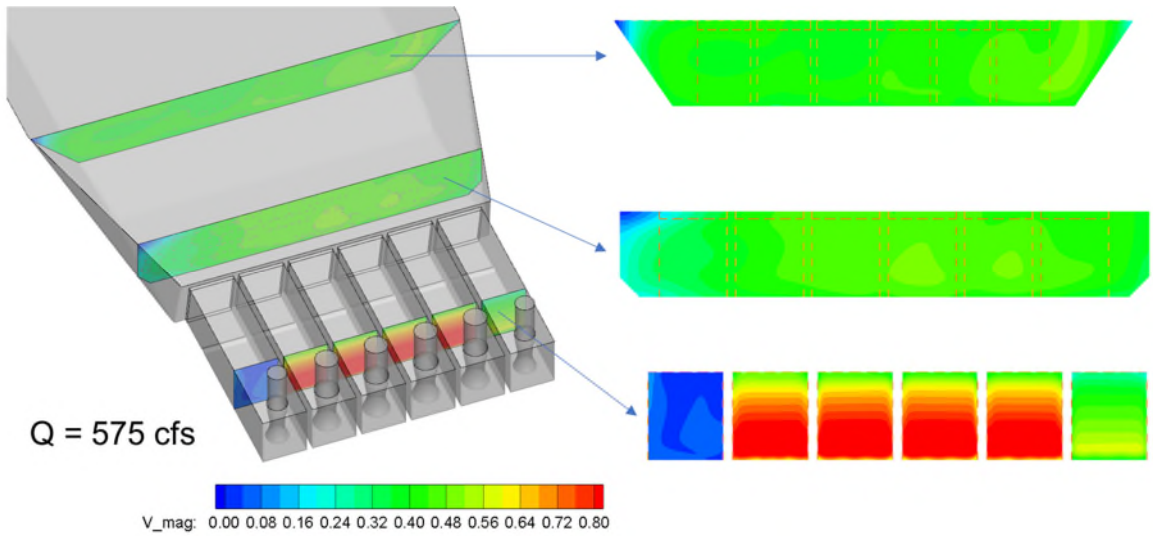

Figure 52. Cross-sectional velocity contours in the approaching canal and in the pump intakes for the S332C proposed design conditions with vanes and a trash rack (cross-sections are oriented looking downstream), Scenario 2

A vortex visualization using 3D streamlines for the proposed design condition with vanes is shown in Figure 54. The sub-surface vortices are clearly evident in this figure. Figure 55 shows the axial velocity distribution for the proposed design conditions at with vanes. Figure 55 confirms that the velocity distribution within each pump bell is centered at the origin.

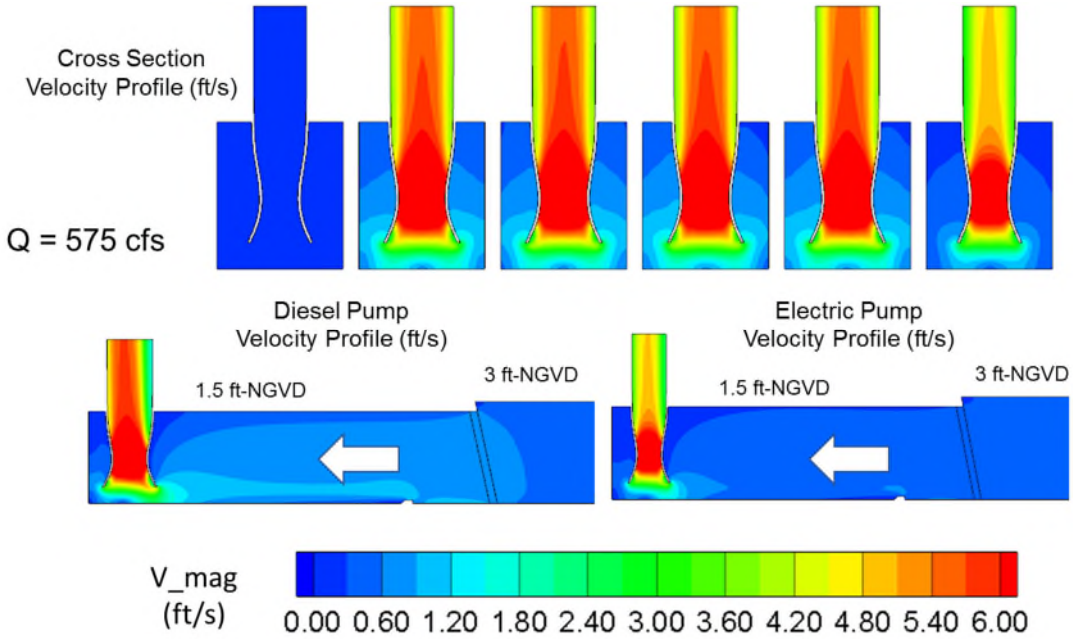

Figure 53. Cross-sectional velocity profiles for the S332C proposed design condition with vanes and a trash rack, Scenario 2

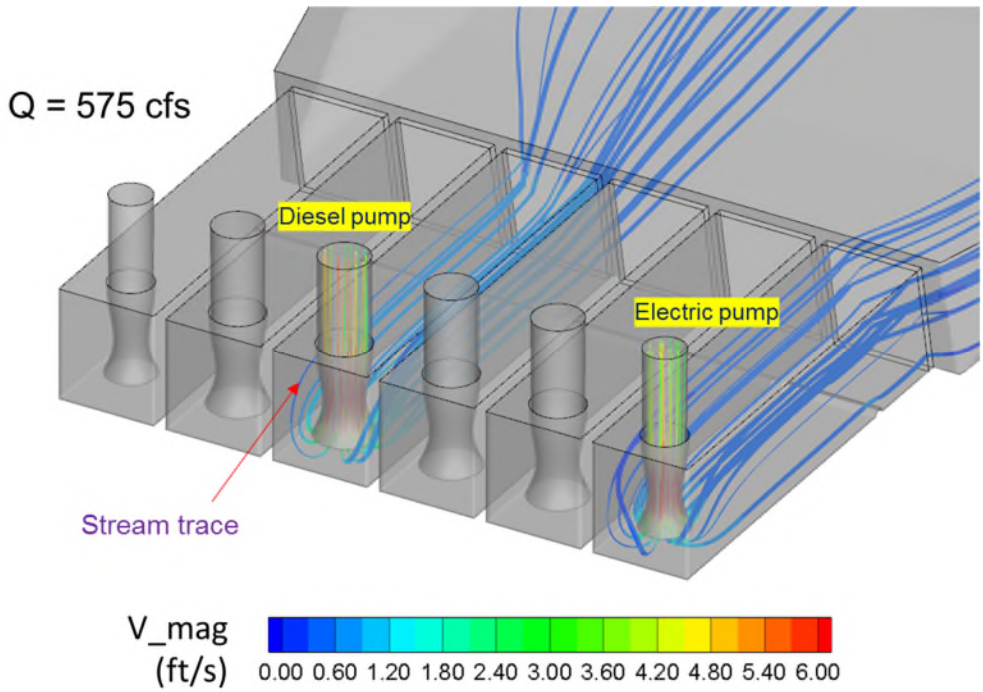

Figure 54. Vortex visualization with 3D streamlines for the S332C proposed design conditions with vanes and a trash rack, Scenario 2

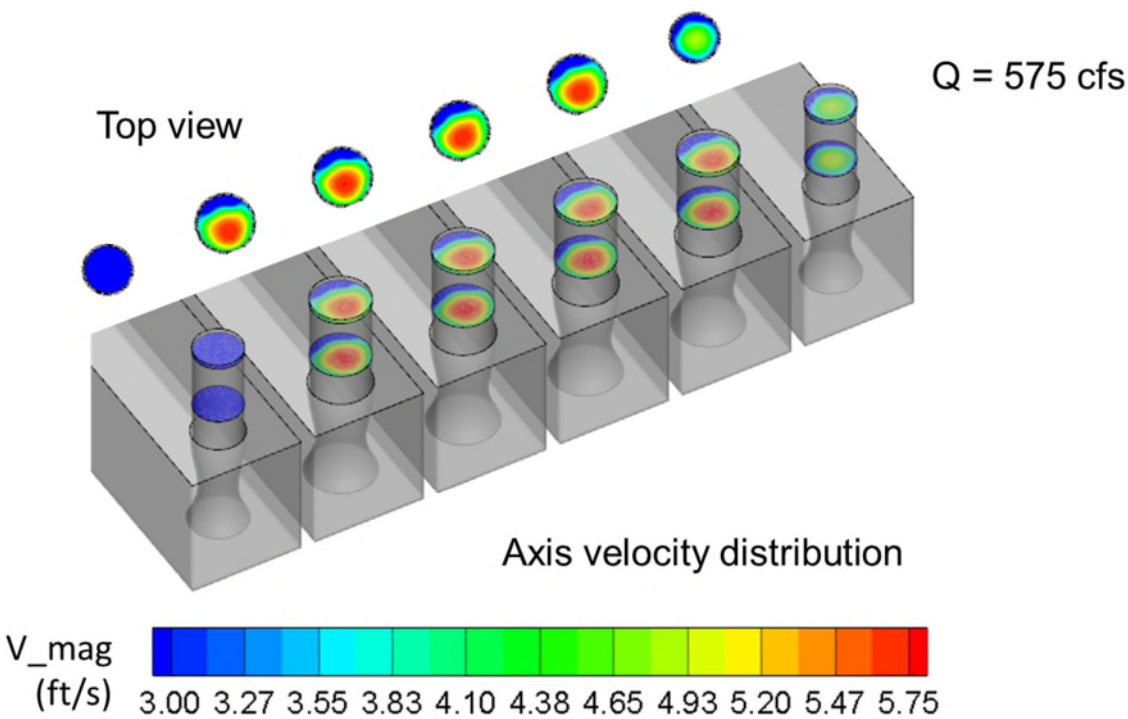

Figure 55. Axial velocity distribution for the S332C proposed design conditions with vanes and a trash rack, Scenario 2

SUMMARY

The proposed replacement pump stations for S332B and S332C are located about 300 feet downstream and 300 feet west of their respective existing locations. For the purposes of this analysis, it was assumed that the layouts and configurations of the replacement pump stations will be similar to those of S357, a permanent pump station. The pump configuration parameters, including the minimum submergence, backwall/floor and sidewall clearances, followed the Hydraulic Institute Standards. The analysis in this report can be summarized as follows:

1) the inflows to each of the existing pump stations as well as to each proposed new pump stations were observed to be biased to one direction if flow separating vanes are not incorporated into the designs;
2) the approach flow and pre-swirl conditions significantly improve with the installation of flow separating vanes and trash racks,
3) forebay flows approaching the pump bells are even, and the flow vortex within each pump column is centered along the vertical axis of symmetry of the pump bell
4) For both S332 B and C, one electric pump unit (75 cfs) is designed as redundancy.
5) The flow fields in the approach channel and in each individual pump column for both 575 cfs and 650 cfs (full capacity) are quite similar.
6) further optimization of both the location and arrangement of pump stations and vanes is needed in the next design phase.

Design Recommendations Table for S332B and S332C

Item	Description
Flow guiding vanes	Vanes near the forebay help avoid imbalance of inflow near intake and eliminate flow bias
Trash rack	Approach flow and pre-swirl conditions significantly improves with trash rack
Station location	300 ft downstream along L-31N canal and 300 ft further west
Pump layout	Four diesel units (125 cfs each), and two electric units (75 cfs each). Electric units to be placed on each ends
Forebay	50 ft, Slope 1:10, Bottom elevation -12.5 ft-NGVD
Floor clearance	2 ft
Backwall clearance	60 inches
Design criteria evaluation	*Approach flow patterns*: even distribution; *Free-surface and sub-surface vortices*: centered at the origin within each pump barrel (non-air entraining); *Velocity distribution at suction bell throat*: flows are even; *Flow pre-swirl*: minimal due to flow separating vanes and trash racks

Steady/unsteady *RANS* models with advanced turbulence closures were determined to be satisfactory for computing complex turbulent flows at both the existing and proposed S332B and S332C pump stations. In the final design phase, if needed, to achieve a higher degree of accuracy, Large Eddy Simulation (LES) turbulence models can be implemented.

REFERENCES

Ansar, M. (1997). "Experimental and Theoretical Studies of Pump Approach Flow Distributions at Water Intakes", Ph.D. Thesis, The University of Iowa, Iowa City, IA.

Carnogurska, M., Prihoda, M., Brestovic, T., Molinek, J., Pyszko, R. (2012). "Determination of permeability and inertial resistance coefficient of filter inserts used in the cleaning of natural gas." *J. Mech. Sci. Technol*. 26(1), 103–111.

Constantinescu, G. and Patel, V. (2000) "Role of turbulence model in prediction of pump-bay vortices." *Journal of Hydraulic Engineering*, 126(5), 387–391.

Constantinescu, S.G. and Patel, V.C. (1998). "Numerical Model for Simulation of Pump Intake Flow and Vortices", *Journal of Hydraulic Engineering*, 124(2), 123-134.

Ergun, S. (1952). "Fluid flow through packed columns." *Chem. Eng. Prog*. 48, 9–94.

Ge, L., and Sotiropoulos, F. (2005). "3D unsteady RANS modeling of complex hydraulic engineering flows. I: Numerical model." *J. Hydraul. Eng.*, 131(9), 800-808.

Ge, L., Lee, S. O., Sotiropoulos, F., and Sturm, T. (2005). "3D unsteady RANS modeling of complex hydraulic engineering flows. II: Model validation and flow physics." *J. Hydraul. Eng.*, 131(9), 809-820.

Geertsma, J. (1974). "Estimating the coefficient of inertial resistance in fluid flow through porous media." *Soc. Petrol. Eng. AIME J*. 14(5), 445–450.

Li, S., Yong, L., Silva, J.M., and Patel V.C. (2001) "CFD Model of Three-Dimensional Flow in Practical Water Pump Intakes", IIHR Technical Report No. 419, The University of Iowa, Iowa City, IA.

Lu, L.G, Cao, Z.G., and Zhou, J.R. (1997). "The Optimum Hydraulic Design of Pump Intakes", Shui Li Xue Bao, Vol. 3, pp. 16-25.

Nielsen, E. J., and Diskin, B. (2017). "High-performance aerodynamic computations for aerospace applications." *Parallel Comput.*, 64, 20-32.

Pradeep, S., Sayantan G., Prasad, P., Mohan Kumar, M. (2012) "CFD simulation and experimental validation of a horizontal pump intake system." *ISH Journal of Hydraulic Engineering*, 18(3), 173–185.

Rajendran, V., Constantinescu, S. and Patel, V. (1999) "Experimental validation of numerical model of flow in pump-intake bays." *Journal of Hydraulic Engineering*, 125(11), 1119–1125.

Tagomori, M. and Gotoh, M. (1989). "Flow Patterns and Vortices in Pump Sump", *International*

Symposium on Large Hydraulic Machinery, Beijing, China.

Takata, I., Kawata, Y., Kobayashi, T., and Morinishi, Y. (1992). "Large-Eddy Simulation of Unsteady Turbulent Swirl Flow in the Pump Intake", *Proceedings of First Computational Fluid Dynamics European Conference*, Brussels, Belgium, Elsevier Press, 255-261.

Tokyay, T. & Constantinescu, S. (2006) "Validation of a large-eddy simulation model to simulate flow in pump intakes of realistic geometry. *Journal of Hydraulic Engineering* 132(12), 1303–1315.

Wang, Y., Politano, M., Ho, H. C., Muste, M., Michell, F., and Stallings, J. (2014). "Assessment of ice plugging of a cooling water intake by a numerical model." *Journal of Hydraulic Research*, 52(1), 81-92.

Zeng, J., Zhang L. Q., Ansar M., Damisse E., and Castro-Gonzalez, J. A. (2016). "Applications of computational fluid dynamics to flow ratings at prototype spillways and weirs. I: Data generation and validation." *J. Irrig. Drain. Eng.*, 143(1), 04016072.

Zhang, J. and Yee, T. (2018). "Extent, capacity and possibilities of computational fluid dynamics as a design tool for pump intakes: A review", *Water Science & Technology: Water Supply*, 18(5), 1518-1530.

Zhao, Q., Misra, S. K., Svendsen, I. A., and Kirby, J. T. (2004). "Numerical study of a turbulent hydraulic jump", *Proc., 17th Engineering Mechanics Conf.*, ASCE, Newark, Delaware.

APPENDIX

Minimum Submergence Calculations

	Bell Diameter	**D (in.) =**	81.6			**Flow Q (cfs)=**	125		V (ft/s)	F
Froude Number based on D,		F_D =	0.23						3.443678	0.232723
						Sc (in.)	Remark		6.351783	0.429253
	British Hydraulic Research Association (Prosser 1977)				**BHRA**	122.4	Sc=1.5D			
	Hydraulic Institute Standards (at 125 cfs)				**HIS (2000)**	105	Sc=D{aF_D^b}, a= 2.23, b =0.38			
Revised Hydraulic Institute Standards (Hecker, 2016, Knauss 1987)					**R-HIS (2016)**	125	Sc=D(a+bF_D), a= 1, b =2.3			
	Floor Clearance	C (in.) =	24.48							
Backwall Clearance		B (in.) =	61.2							

S = Submergence above inlet bell entrance
D = Inlet bell O.D.
F_D = Froude number = $V/(gD)^{0.5}$
V = Velocity at inlet bell face = flow/area using O.D.
g = Acceleration due to gravity

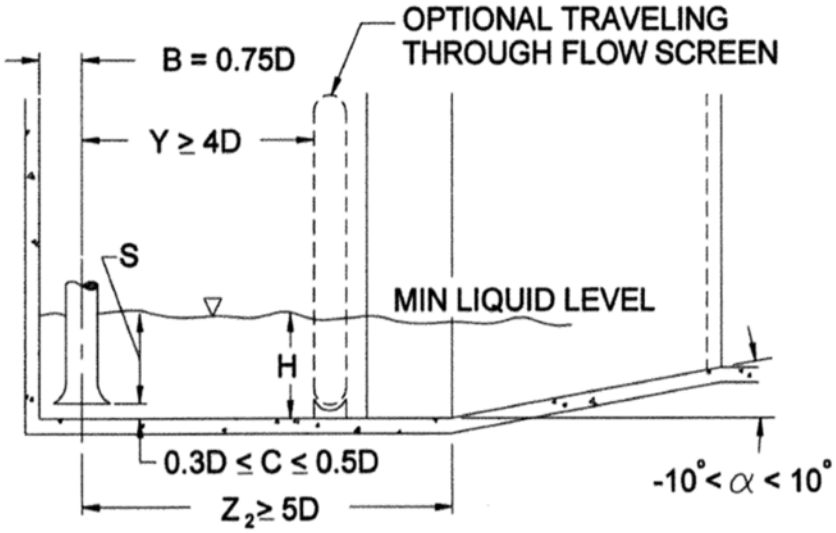

Figure A1. Recommended intake structure layout (*Courtesy*: Hydraulic Institute)

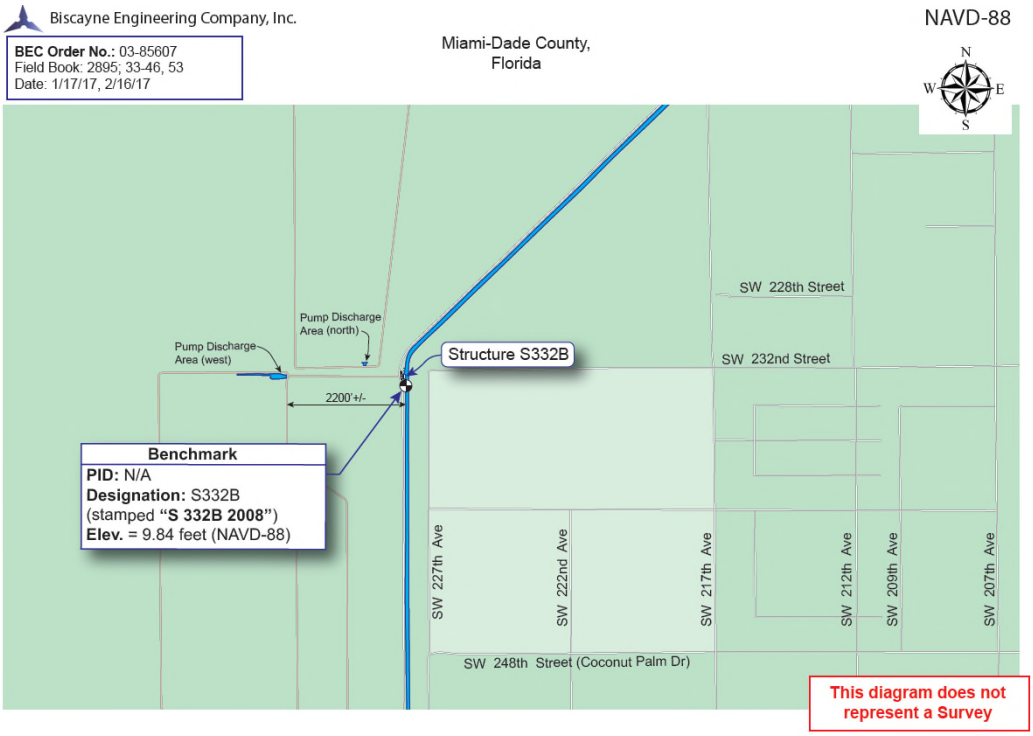

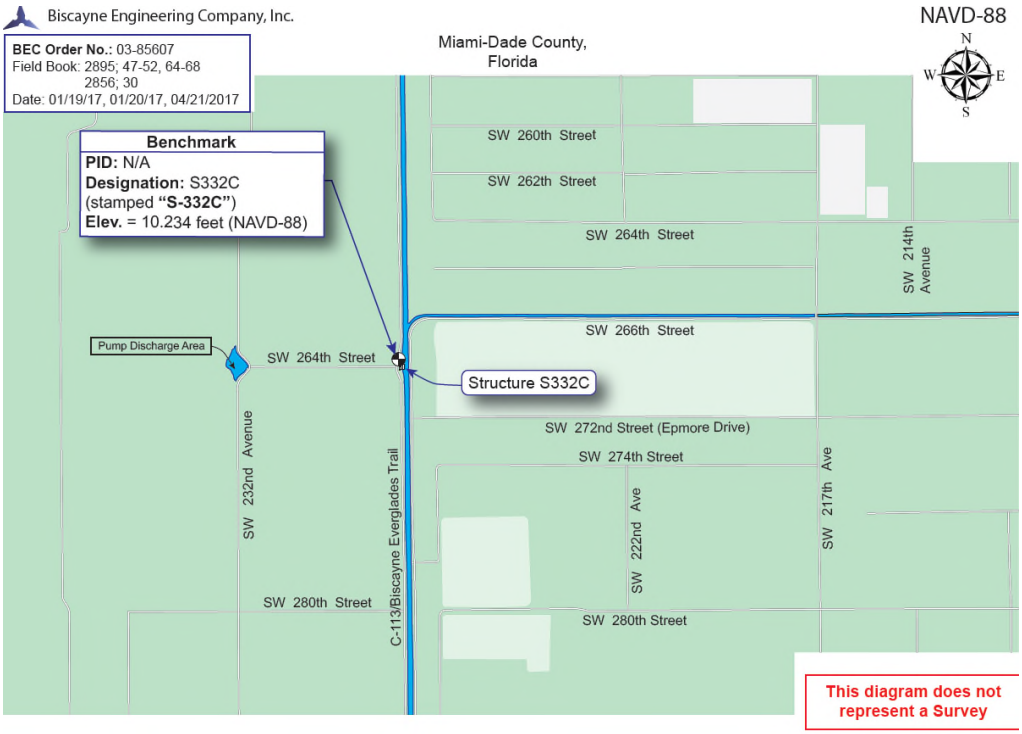

Figure A2. Locations of S332B and S332C pump stations

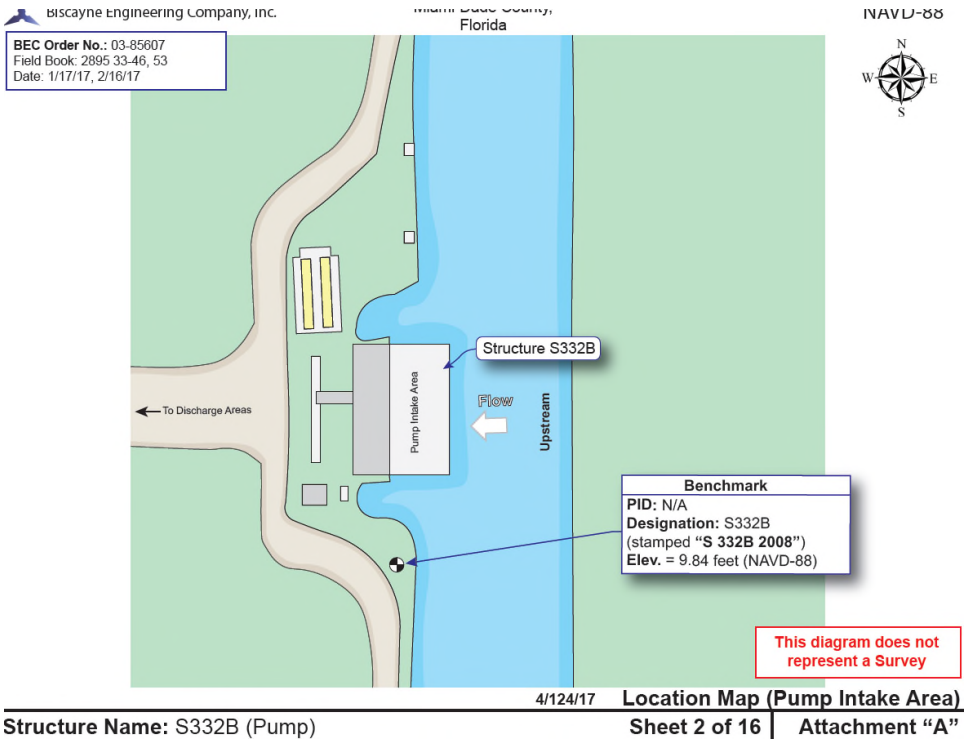

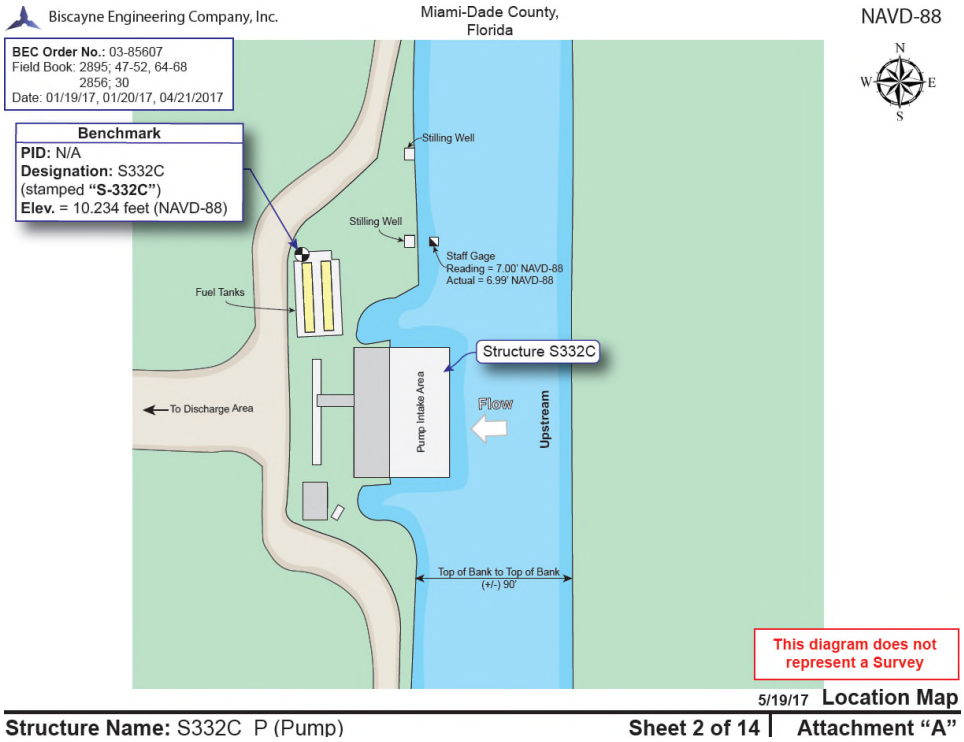

Figure A3. Pump details of existing S332B and S332C pump stations

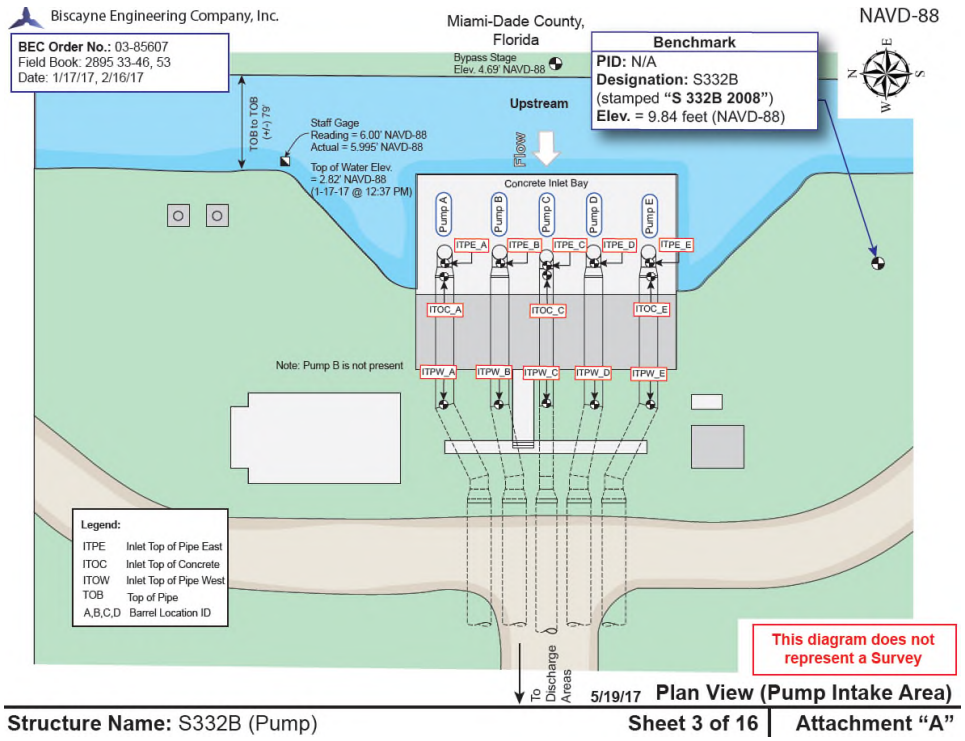

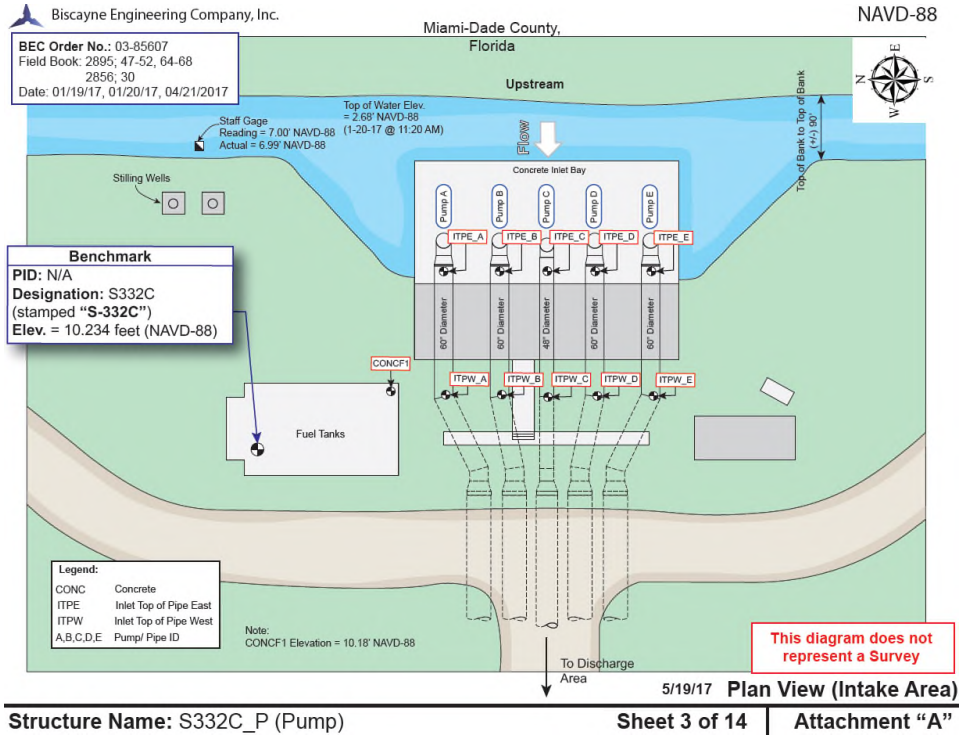

Figure A4. Pump arrangement of existing S332B and S332C pump stations

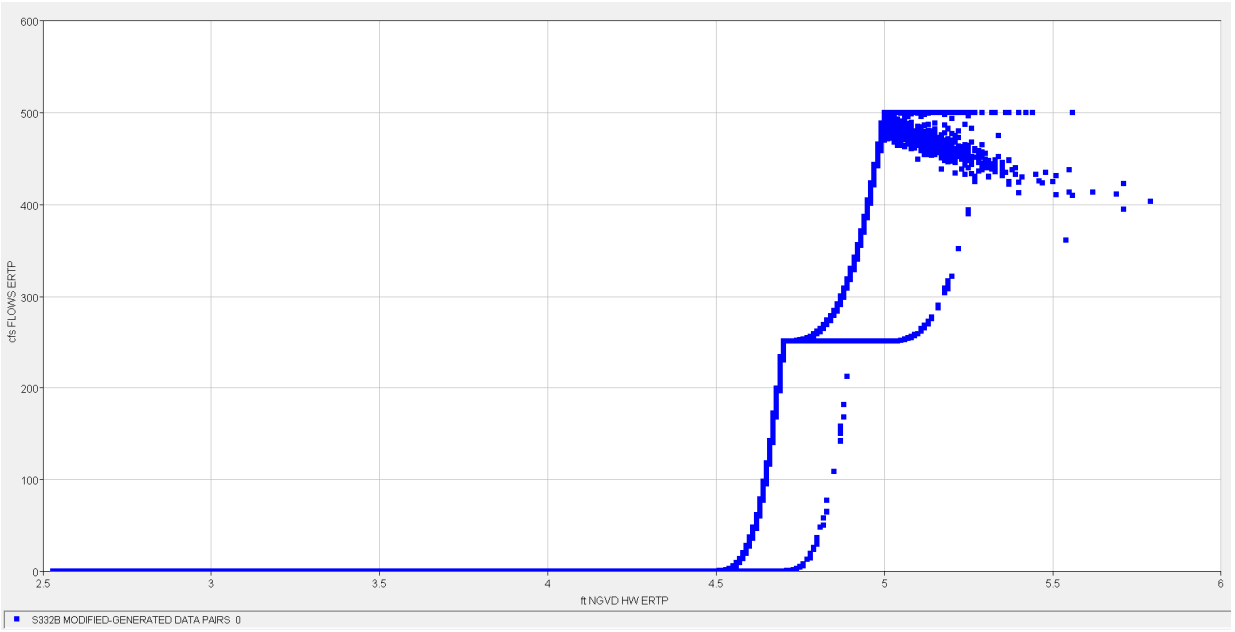

Figure A5. S332B HW versus Flow, ERTP

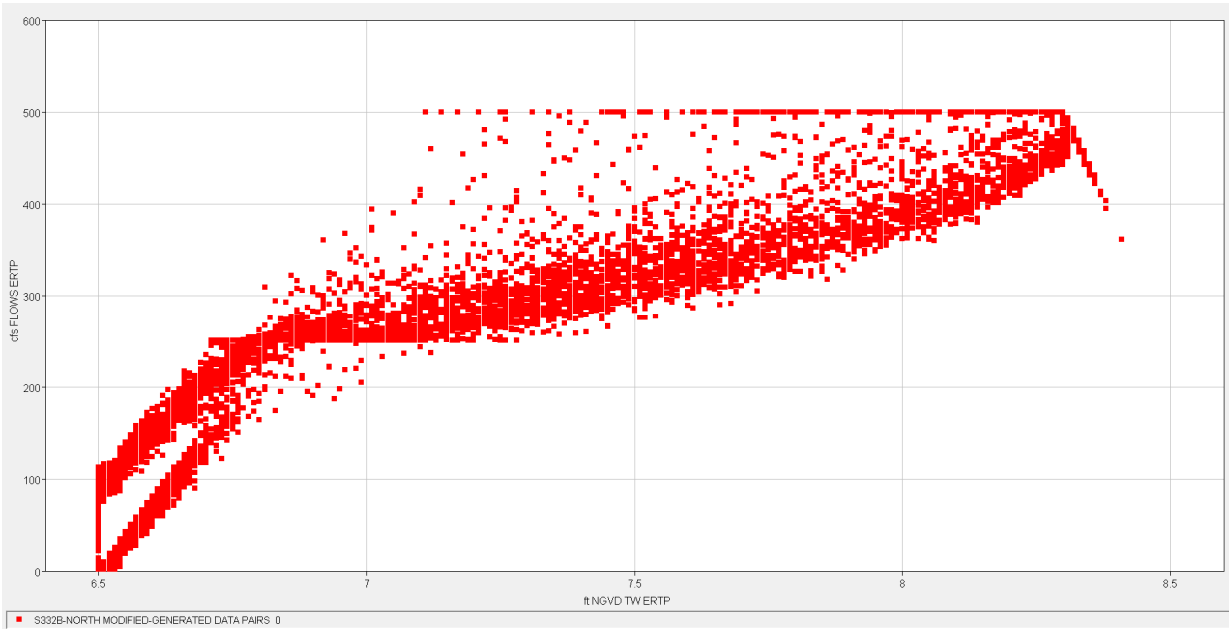

Figure A6. S332B TW Northern Detention Area (NDA) versus Flow, ERTP

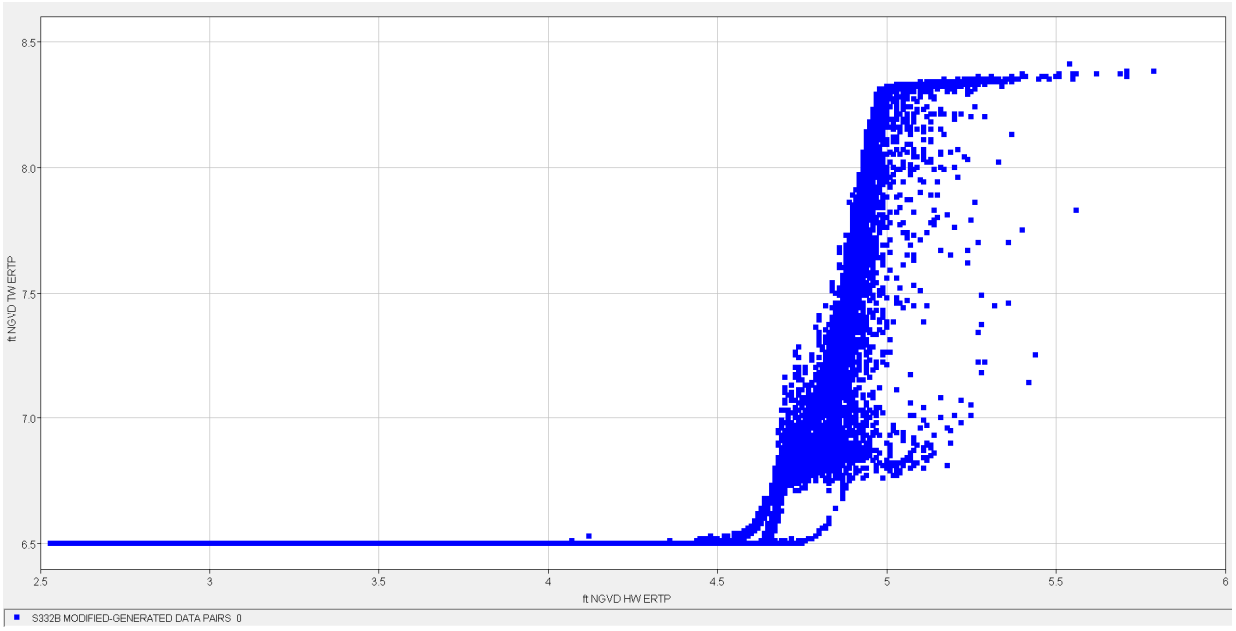

Figure A7. S332B HW versus TW Northern Detention Area (NDA), ERTP

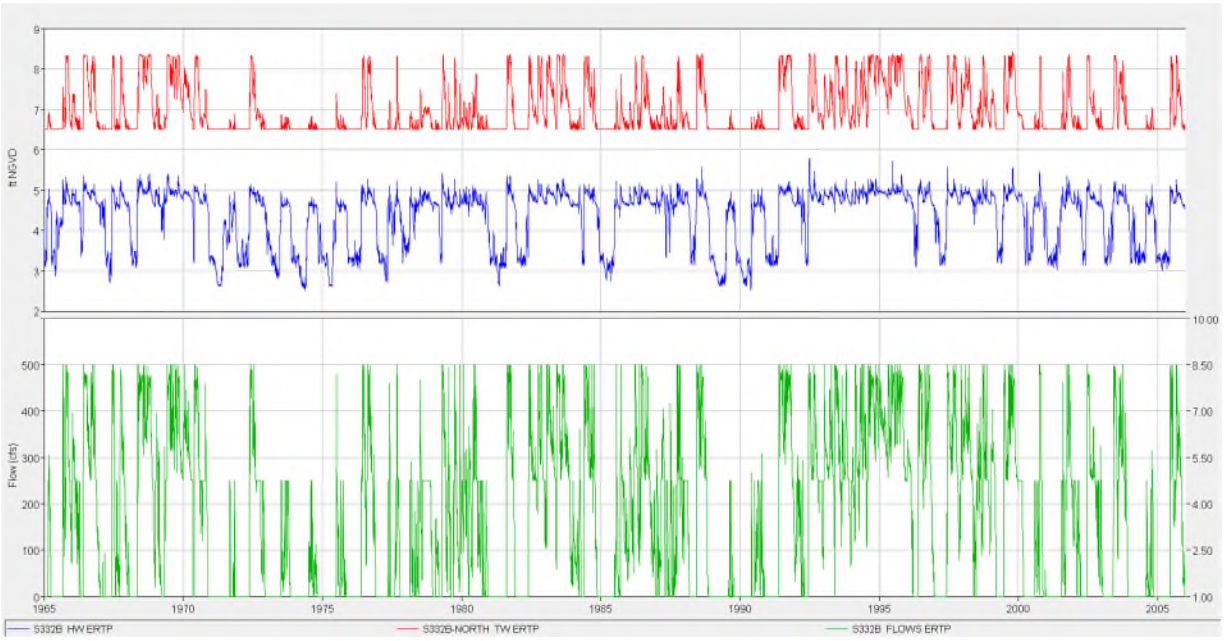

Figure A8. Historical discharge and stage data at S332B, ERTP